

# 1 Atmospheric ammonia and particulate inorganic nitrogen 2 over the United States

3  
4 C.L. Heald<sup>1</sup>, J.L. Collett Jr.<sup>2</sup>, T. Lee<sup>2</sup>, K. B. Benedict<sup>2</sup>, F. M. Schwandner<sup>2,\*</sup>, Y. Li<sup>2</sup>,  
5 L. Clarisse<sup>3</sup>, D. R. Hurtmans<sup>3</sup>, M. Van Damme<sup>3</sup>, C. Clerbaux<sup>3,4</sup>, P.-F. Coheur<sup>3</sup>, S.  
6 Philip<sup>5</sup>, R.V. Martin<sup>5</sup>, H. O. T. Pye<sup>6</sup>

7 [1]{Department of Civil and Environmental Engineering and Department of Earth,  
8 Atmospheric and Planetary Sciences, MIT, Cambridge, MA, USA }

9 [2]{Department of Atmospheric Science, Colorado State University, Fort Collins, CO, USA }

10 [3]{Spectroscopie de l'Atmosphère, Service de Chimie Quantique et Photophysique,  
11 Université Libre de Bruxelles, Brussels, Belgium }

12 [4]{UPMC Univ. Paris 06; Université Versailles St-Quentin; CNRS/INSU, LATMOS-IPSL,  
13 Paris, France }

14 [5]{Department of Physics and Atmospheric Science, Dalhousie University, Halifax, Canada }

15 [6]{U.S. Environmental Protection Agency, Research Triangle Park, NC, USA }

16 [\*]{now at: Earth Observatory of Singapore, Nanyang Technological University, Singapore }

17 Correspondence to: C. L. Heald (heald@mit.edu)

## 18 19 **Abstract**

20 We use in situ observations from the Interagency Monitoring of PROtected Visual  
21 Environments (IMPROVE) network, the Midwest Ammonia Monitoring Project, 11 surface  
22 site campaigns as well as Infrared Atmospheric Sounding Interferometer (IASI) satellite  
23 measurements with the GEOS-Chem model to investigate inorganic aerosol loading and  
24 atmospheric ammonia concentrations over the United States. IASI observations suggest that  
25 current ammonia emissions are underestimated in California and in the springtime in the  
26 Midwest. In California this underestimate likely drives the underestimate in nitrate formation  
27 in the GEOS-Chem model. However in the remaining continental United States we find that  
28 the nitrate simulation is biased high (normalized mean bias  $\geq 1.0$ ) year-round, except in

1 Spring (due to the underestimate in ammonia in this season). None of the uncertainties in  
2 precursor emissions, the uptake efficiency of  $N_2O_5$  on aerosols, OH concentrations, the  
3 reaction rate for the formation of nitric acid, or the dry deposition velocity of nitric acid are  
4 able to explain this. We find that reducing nitric acid concentrations to 75% of their simulated  
5 values corrects the bias in nitrate (as well as ammonium) in the U.S. However the mechanism  
6 for this potential reduction is unclear and may be a combination of errors in chemistry,  
7 deposition and sub-grid near-surface gradients. This “updated” simulation reproduces PM and  
8 ammonia loading and captures the strong seasonal and spatial gradients in gas-particle  
9 partitioning across the United States. We estimate that nitrogen makes up 15-35% of  
10 inorganic fine PM mass over the U.S., and that this fraction is likely to increase in the coming  
11 decade, both with decreases in sulfur emissions and increases in ammonia emissions.

12

## 13 **1 Introduction**

14 Ammonia ( $NH_3$ ) is the most abundant form of gas-phase reduced nitrogen in the atmosphere  
15 and contributes to both the formation of particulate matter (PM) and the deposition of reactive  
16 nitrogen to the environment. Particulate matter in the atmosphere degrades air quality and  
17 visibility and can modify the radiative balance of the Earth both directly and indirectly  
18 through the formation of cloud droplets. Human morbidity has been shown to increase  
19 linearly with PM concentrations (Dockery et al., 1993; Pope et al., 2009), suggesting that  
20 while air quality standards are set to protect human health, there are no “safe” levels of PM.  
21 Typically over half of the fine PM in the United States is made up of inorganic aerosol  
22 (defined here as the sum of: sulfate, nitrate and ammonium) (NARSTO, 2004). These aerosols  
23 are formed in the atmosphere from gas-phase precursors (sulfur dioxide, nitrogen oxides and  
24 ammonia), which are largely emitted from anthropogenic activity, including agriculture. The  
25 formation of these aerosols is thermodynamically linked, with ammonium nitrate formation  
26 generally taking place only when sulfate has been fully neutralized. Ammonia sources have  
27 increased through the 20<sup>th</sup> century with industrial fertilizer production (Erisman et al., 2008),  
28 provoking concerns regarding excess nitrogen deposition to sensitive ecosystems (Beem et  
29 al., 2010). Recent trends in wet deposition and air quality indicate that the relative role of  
30 reduced vs oxidized nitrogen is changing (Pinder et al., 2011). Thus ammonia and particulate  
31 nitrogen play important roles in both air quality and ecosystem health.

1 Model studies suggest that the reduction of SO<sub>2</sub> emissions in the U.S. may shift aerosol  
2 composition towards nitrate formation (eg. (Pye et al., 2009)) and that ammonia emissions  
3 control could play an increasing role in achieving compliance with air quality standards  
4 (Pinder et al., 2008;Pinder et al., 2007). While such predictions are predicated on accurate  
5 model descriptions of both ammonia and the complete inorganic gas-particle system, there  
6 have been few observational constraints available to verify the fidelity of these models. This  
7 is largely the result of the challenges of measuring ammonia, a sticky, semi-volatile  
8 compound with ambient concentrations that vary over several orders of magnitude (von  
9 Bobruzki et al., 2010). Model simulations have been widely validated against surface  
10 network observations of inorganic aerosol concentrations and wet deposition (eg. (Park et al.,  
11 2004;Adams et al., 1999;Bessagnet et al., 2004)). Observations of gas-phase precursors  
12 alongside aerosol concentrations are more rare. Efforts have been made to optimize inorganic  
13 aerosol precursor emissions based on observed particle concentrations (Henze et al., 2009),  
14 however errors in PM formation and loss may cloud the links between precursor emissions  
15 and ambient particle concentrations. Recently, infrared satellite instruments have  
16 demonstrated the capability to measure ammonia from space (Beer et al., 2008;Clarisse et al.,  
17 2009). The spatial and continuous global coverage of such observations provides critical  
18 complementarity to specific field campaign observations. However, the sensitivity of these  
19 infrared sounders can be limited, particularly as atmospheric ammonia is largely present in the  
20 boundary layer, where thermal contrast can be low. Our goal here is to apply a series of  
21 unique satellite and surface inorganic measurements to investigate both atmospheric ammonia  
22 and particle phase nitrogen in the United States.

23 Thermodynamic models have been developed to describe the partitioning of semi-volatile  
24 species. Several studies have confirmed that the assumption of equilibrium partitioning is  
25 valid for ambient aerosol (eg (Ellis et al., 2011;Nowak et al., 2010;Nowak et al., 2006)). Thus  
26 3-D model simulation errors are not likely to result from errors in the description of  
27 thermodynamic partitioning but rather from (1) errors in precursor emission estimates (2)  
28 errors in formation of sulfate or nitric acid (3) biases in temperature and humidity leading to  
29 biased gas-particle partitioning or (4) errors in gas and particle deposition. Here we  
30 investigate the skill of the GEOS-Chem global model in reproducing regional ammonia  
31 loadings and inorganic concentrations and partitioning. We note that the study of Walker et al,  
32 (2012), completed at the same time as this work, addresses some of the same issues,  
33 particularly in California, and reports similar results to those presented here. Our objective is

1 to identify obvious biases in the key processes outlined above and to suggest what kind of  
2 field measurements could be particularly valuable. Routine measurement of ammonia will be  
3 added in the coming years to select sites in the IMPROVE network in the United States,  
4 providing additional constraints on inorganic gas-particle partitioning. These future  
5 observations and those discussed herein can contribute to an improved understanding of the  
6 complete inorganic system. This will be critical to the accurate interpretation of new satellite  
7 observations of ammonia and resulting estimates of the role of nitrogen in PM formation,  
8 climate, and ecosystem health.

## 9 10 **2 Measurement Description**

### 11 **2.1 IMPROVE network aerosol measurements and the Midwest Ammonia** 12 **Monitoring Project**

13 The Interagency Monitoring of PROtected Visual Environments (IMPROVE) network of  
14 stations was established in 1987 to monitor visibility in national parks and other protected  
15 environments in the United States (Malm et al., 1994). Surface concentrations of fine particle  
16 ( $PM_{2.5}$ ) sulfate, nitrate, organic carbon and elemental carbon are measured as 24-hour  
17 averages every third day. The ammonium ion is not routinely measured in the IMPROVE  
18 network. Nitrate (and sulfate) are collected on a Nylasorb substrate after passing through a  
19 carbonate denuder tube, minimizing both nitrate volatilization and gas-phase contamination  
20 (Malm et al., 2004). We show here comparisons at 238 sites operating in 2004 in the  
21 continental United States.

22 We also examine measurements from the Midwest Ammonia Monitoring Project (MWNH<sub>3</sub>),  
23 a field intensive at 10 sites (9 co-located at IMPROVE sites) from November 2003 through  
24 October 2005 (Blanchard and Tanenbaum, 2005; Sweet et al., 2005). We show only  
25 measurements from 2004. Measurements of fine particle sulfate, nitrate, ammonium as well  
26 as gas-phase ammonia, nitric acid and sulfuric acid were collected every 6<sup>th</sup> day by the Illinois  
27 State Water Survey. The measurement system consisted of two denuders, one to collect HNO<sub>3</sub>  
28 and SO<sub>2</sub> and the second to collect NH<sub>3</sub>, followed by a Teflon and Nylon filter to collect the  
29 particles. Measured sulfate & nitrate agreed well with co-located IMPROVE measurements  
30 (Blanchard and Tanenbaum, 2005).

31

## 1 **2.2 In situ measurements**

2 Several field experiments were designed and conducted to investigate the chemical  
3 composition of PM<sub>2.5</sub> aerosol and the concentrations of trace gases (HNO<sub>3</sub>, NH<sub>3</sub> and SO<sub>2</sub>) at  
4 monitoring locations for the IMPROVE program from the late 1990's through 2010 (Figure  
5 1). Daily 24-hr measurements were made in a variety of seasons during 1999, 2002, 2003 and  
6 2004. Study sites included Big Bend National Park (July – October, 1999), Yosemite National  
7 Park (July – September, 2002), Bondville, Illinois (February 2003), San Geronio Wilderness  
8 Area, California (April and July 2003), Grand Canyon National Park, Arizona (May 2003),  
9 Brigantine National Wildlife Refuge, New Jersey (November 2003), and Great Smoky  
10 Mountains National Park, Tennessee (July/August 2004). Aerosol composition measured at  
11 these sites has previously been reported (Yu et al., 2005b; Lee et al., 2004; Lee et al., 2008a; Yu  
12 et al., 2006). In addition, a series of year-long intensive measurements were made in Rocky  
13 Mountain National Park (Nov 2008-Oct 2009, daily), Boulder, WY (Dec 2006-December  
14 2010, 3&4-day average), and Brush and Loveland, CO (Dec 2008-Nov 2009, weekly  
15 average).

16 A URG (University Research Glassware) cyclone/annular denuder/filter pack system was  
17 used for PM<sub>2.5</sub> and trace gas (HNO<sub>3</sub>, NH<sub>3</sub> and SO<sub>2</sub>) sampling. Ambient air is drawn into the  
18 URG sampler through a cyclone (D<sub>50</sub>=2.5 μm, 10 LPM), and through two denuders in series  
19 for collection of the gaseous species of interest. Na<sub>2</sub>CO<sub>3</sub> (or NaCl for Big Bend NP and  
20 Boulder, WY) coated the first denuder for collection of gaseous HNO<sub>3</sub> and SO<sub>2</sub> and the  
21 second denuder was coated with phosphorus acid (or citric acid for Big Bend NP) to collect  
22 gaseous NH<sub>3</sub>. SO<sub>2</sub> concentrations are not measured at Big Bend NP and in Boulder, WY. The  
23 air stream continued through either a nylon filter (Nylasorb, 1.0 μm pore size, Pall  
24 Corporation) and a backup phosphorus acid-coated denuder or a 3-stage filter pack with a  
25 Teflon filter (Teflo, 2.0 μm pore size, Pall Corporation), a nylon filter (Nylasorb, 1.0 μm pore  
26 size, Pall Corporation) and a backup citric acid-coated cellulose filter (or quartz filter).  
27 Sampling at the ammonia-rich Brush, CO site was performed with a lower flow rate (3 LPM)  
28 and with an extra ammonia denuder before the filter to ensure that ammonia collection  
29 capacity was not exceeded. Analysis of PM<sub>2.5</sub> filter and denuder extracts focused on the main  
30 PM<sub>2.5</sub> ionic species (SO<sub>4</sub><sup>2-</sup>, NO<sub>3</sub><sup>-</sup>, NH<sub>4</sub><sup>+</sup>), and trace gases (HNO<sub>3</sub>, NH<sub>3</sub> and SO<sub>2</sub>). Sampling and  
31 analysis details are described in detail elsewhere (Yu et al., 2005b; Lee et al., 2004; Lee et al.,  
32 2008b). Species detection limits were typically 20-70 ngm<sup>-3</sup> while measurement precisions

1 were typically in the range of 3-9% (RSD) for individual samples, but are correspondingly  
2 smaller for the monthly or seasonal means shown here. Accuracy checks on key components  
3 of the measurement (sample volume, extract volume, and ion concentration) typically reveal  
4 biases of a few percent, with a range from approximately 1-10%. PM<sub>2.5</sub> ion concentrations  
5 measured with the URG compare well ( $R^2 > 0.9$  and mean biases less than 10% across the US)  
6 with online measurements, as discussed by Lee et al. (2008b).

7

### 8 **2.3 Infrared Atmospheric Sounding Interferometer (IASI)**

9 The Infrared Atmospheric Sounding Interferometer (IASI) was launched aboard the MetOp-A  
10 platform in October 2006. This nadir sounder provides global measurements of a suite of  
11 atmospheric trace gases, including ammonia (Clerbaux, 2009). The instrument footprint (12  
12 km x 12 km) is combined with extensive cross-track scanning (2200 km) to provide detailed  
13 global daily coverage. Measurements from sun-synchronous polar orbit are made twice daily  
14 at 9:30 and 21:30 local time.

15 Ammonia retrievals are based on an absorption feature  $\sim 950 \text{ cm}^{-1}$ . Initial global retrievals  
16 reported by *Clarisse et al.* (2009) were based on a brightness temperature scaling approach,  
17 but here retrievals apply formal optimal estimation methods (Rodgers, 2000) to retrieve the  
18 profile of ammonia ( $\hat{\mathbf{x}}$ ):

$$19 \quad \hat{\mathbf{x}} = \mathbf{x}_a + \mathbf{A}(\mathbf{x} - \mathbf{x}_a) + \varepsilon \quad (1)$$

20 where  $\mathbf{x}$  is the true profile,  $\mathbf{x}_a$  is the a priori constraint, which is a constant global moderately  
21 polluted mean profile from the TM5 model, and  $\varepsilon$  is the spectral measurement error. The  
22 averaging kernels ( $\mathbf{A}$ ) describe the vertical sensitivity of the instrument and depend on the  
23 thermal contrast and vertical distribution of ammonia. IASI NH<sub>3</sub> measurements are generally  
24 most sensitive at 1-2 km altitude, where concentrations are highest and thermal contrast  
25 sufficient for detection. Thermal contrast is also highest during daytime, and therefore only  
26 daytime retrievals are used here. Retrieved ammonia is shown here as an integrated column  
27 concentration given the low vertical sensitivity.

28 The retrievals are performed in near real time using the fast radiative transfer model FORLI  
29 (Hurtmans et al., 2012). Note that with the constraints applied to allow for global retrievals,  
30 the averaging kernels and degrees of freedom (DOF) are unrealistically small for this research

1 product (typically  $< 0.3$  over the continental United States), especially in comparison to the  
2 initial work of Clarisse et al.(2010) over the San Joaquin Valley. This does not impact the  
3 quality of the retrievals; however, low DOFs imply larger reliance on the a priori when  
4 attempting to compare the IASI retrievals with other measurements or models. This is  
5 discussed further in Section 4.2.

6

### 7 **3 Model Description**

8 We compare here measurements of the inorganic gas-particle system with the GEOS-Chem  
9 global model of atmospheric chemistry ([www.geos-chem.org](http://www.geos-chem.org)). We employ v9-01-01 of the  
10 model driven by GEOS-5 assimilated meteorology from the NASA Global Modeling and  
11 Assimilation Office (GMAO). We conduct a series of coupled oxidant-aerosol nested grid  
12 simulations ( $0.5^\circ \times 0.67^\circ$  horizontal resolution) (Chen et al., 2009) over North America for  
13 three years (2004, 2009 and 2010) and show results over the continental United States.  
14 Boundary conditions are from global simulations performed at  $2^\circ \times 2.5^\circ$  horizontal resolution  
15 for the same years.

16 The GEOS-Chem oxidant-aerosol simulation includes  $\text{H}_2\text{SO}_4\text{-HNO}_3\text{-NH}_3$  aerosol  
17 thermodynamics coupled to an ozone- $\text{NO}_x$ -hydrocarbon-aerosol chemical mechanism (Park et  
18 al., 2004). Partitioning of total ammonia and nitric acid between the gas and particle phases is  
19 calculated using the ISORROPIA II thermodynamic equilibrium model (Fountoukis and  
20 Nenes, 2007) as implemented in GEOS-Chem by *Pye et al.* (2009). The gas-particle  
21 equilibrium considers sodium and chloride from accumulation mode sea salt as well as  
22 sulfate, nitrate and ammonium. Formation of inorganic aerosol on coarse mode dust and sea  
23 salt is excluded, thus estimated aerosol concentrations represent  $\text{PM}_{2.5}$  concentrations. In this  
24 implementation of ISORROPIA the inorganic aerosol are assumed to be metastable on the  
25 upper branch of the hygroscopicity hysteresis curve. The metastable assumption likely holds  
26 near the surface where relative humidities exceed the deliquescence relative humidity on a  
27 daily basis, but may not be appropriate in the free troposphere (Wang et al., 2008).

28 Anthropogenic emissions of aerosol precursors over the US are specified according to the US  
29 EPA National Emission Inventory for 2005 (NEI05, with seasonality as in Park et al. (2004)),  
30 with biofuel emissions from the US EPA National Emission Inventory for 1999 (NEI99) and  
31 year-specific biomass burning from the GFED2 inventory (van der Werf et al., 2006).

1 Anthropogenic emissions are scaled to the model year following national energy use statistics  
2 as described by van Donkelaar et al. (2008). Natural and agricultural ammonia emissions in  
3 GEOS-Chem follow the global inventory of *Bouwman et al.* (1997) with seasonal variation as  
4 described by *Park et al.* (2004). Natural emissions of DMS, NO<sub>x</sub> from lightning and soils, and  
5 sea salt depend on meteorology and are computed online in the model (see description in Pye  
6 et al. (2009)). Emission totals for ammonia, NO<sub>x</sub> and SO<sub>x</sub> over the United States for 2004 are  
7 given in Table 1.

8 Wet deposition of soluble aerosols and gases follows the scheme of *Liu et al.* (2001) including  
9 contributions from scavenging in convective updrafts, rainout, and washout. Dry deposition  
10 follows a standard resistance-in-series model (Wesely, 1989) and is discussed further in  
11 Section 4.3.

12 The GEOS-5 meteorology fields used here suffer from an artificially low planetary boundary  
13 layer (PBL) height at nighttime which can produce large biases in simulated nighttime surface  
14 concentrations (and thus 24-hr or monthly means). We implement a correction to the standard  
15 v9.01.01 version of GEOS-Chem by restricting the PBL height from dropping below a  
16 minimum mechanical mixing depth, defined as a function of local friction velocity (Lin and  
17 McElroy, 2010;Koracin and Berkowicz, 1988). This restriction brings PBL heights in line  
18 with values measured at the ARM-Southern Great Plains site (not shown). This also  
19 eliminates an erroneously large increase in nitrate concentrations at night.

20 Previous studies using GEOS-Chem and the MARS-A thermodynamic scheme have shown  
21 large biases (up to a factor of two) in simulated nitrate over the United States (Park et al.,  
22 2004;Henze et al., 2009). Recent evaluation of the inorganic aerosol simulation using  
23 ISORROPIA also shows large biases in nitrate, which is overestimated by GEOS-Chem in the  
24 Eastern U.S. and underestimated in the Western US (Pye et al., 2009). Zhang et al. (2012),  
25 using a similar model configuration to our work (but using the MARS-A scheme), show that  
26 both nitric acid and ammonium nitrate concentrations are overestimated in the model when  
27 sulfate is unbiased, particularly in wintertime. They suggest that this is the result of excessive  
28 HNO<sub>3</sub> formation via N<sub>2</sub>O<sub>5</sub> hydrolysis. In addition, they show that ammonia measurements in  
29 the upper Midwest support an increase in springtime emissions compared to the standard  
30 seasonality applied in GEOS-Chem based on Park et al. (2004).

31 We build on this work by bringing new measurements of both ammonia (satellite) and gas-  
32 particle partitioning (*in situ*) to bear on the inorganic system. We evaluate daily mean

1 concentrations simulated for 2004 with the URG observations from 1999, 2002, 2003 and  
2 2004 described in Section 2. Thus interannual variability in meteorology may degrade the  
3 comparison, particularly the ability to reproduce daily variability. The same 2004 simulation  
4 is compared to monthly mean measurements across the IMPROVE network and the Midwest  
5 Ammonia Monitoring Project. Monthly mean measurements from 2009 in Wyoming and  
6 Colorado are compared to the 2009 simulation. For comparison with IASI measurements we  
7 match simulated ammonia profiles with the location and time of each retrieval and then apply  
8 the IASI averaging kernel and a priori ammonia profile as in equation 1, and integrate over  
9 the vertical column. The paired comparisons are then re-gridded to the GEOS-Chem  
10 horizontal resolution.

11

## 12 **4 Results**

### 13 **4.1 Initial fine PM evaluation**

14 The over 200 IMPROVE stations reporting surface  $PM_{2.5}$  composition in 2004 provide dense  
15 coverage of the United States and a good basis for model evaluation. Figure 2 shows that the  
16 model reproduces the spatial and seasonal distribution of observed sulfate in 2004, with a  
17 small positive bias in the Northeast in the summer/fall (responsible for the normalized mean  
18 bias of 0.30 in the Fall;  $NMB = \sum_i M_i - O_i / \sum_i O_i$ , where  $O_i$ =observed values and  $M_i$ =model  
19 values) and a small underestimate in the Southeast in summertime. However regression slopes  
20 between observed and simulated means are close to unity, with the exception of the Northeast  
21 in the fall, and thus these errors do not substantially degrade the model simulation of PM.

22 Figure 3 shows the same comparison for nitrate. The model captures the large scale patterns  
23 and seasonality, with two obvious, significant biases. Nitrate concentrations are  
24 underestimated in California, possibly due to an underestimate of ammonia or nitrogen oxide  
25 emissions in the region. The model underestimate of nitrate in the southwest may also be  
26 associated with the failure to represent coarse mode nitrate on dust, the tail of which Lee et al.  
27 (2008a) show can be included in  $PM_{2.5}$  measurements. Nitrate concentrations are  
28 overestimated in the rest of the United States year-round. This is consistent with the  
29 overestimate reported in other studies using both GEOS-Chem and other models (Pye et al.,  
30 2009; Henze et al., 2009; Zhang et al., 2012; Yu et al., 2005a; Walker et al., 2012). Note that  
31 regression lines and NMB statistics are shown separately for the Eastern and Western U.S. to

1 demonstrate these differences. In the Eastern United States normalized mean biases are close  
2 to or greater than 1.0 in all seasons, except spring. Similar biases are seen with respect to  
3 CASTNet network observations of both nitrate and ammonium (not shown here, but reported  
4 by Zhang et al. (2012)). However CASTNet measurements do not provide a good quantitative  
5 test of the fine PM simulation given that measurements may include contamination from  
6 coarse mode nitrate (no size-selective sampling) which can be significant (Lee et al., 2008a),  
7 and CASTNet ammonium nitrate measurements are more susceptible to re-volatilization  
8 errors from the Teflon filters used (Ames and Malm, 2001).

9 Potential causes for the nitrate overestimate seen in Figure 3 include (1) overestimated  
10 precursor emissions of either ammonia or nitrogen oxides (2) excess nitric acid formation (3)  
11 an underestimate in nitrate (or nitric acid) deposition (4) a cold or wet bias in the model that  
12 favors excess ammonium nitrate formation or (5) the absence of  $\text{HNO}_3$  reactions with coarse  
13 mode PM. We explore the bias in simulated nitrate in the following sections.

14

## 15 **4.2 Investigating ammonia emissions**

16 Extensive evaluation in the U.S. against aircraft and satellite observations effectively  
17 precludes errors in  $\text{NO}_x$  emissions as the source of the observed nitrate bias (Lamsal et al.,  
18 2011;Zhang et al., 2012;Martin et al., 2006). However, ammonia emissions are poorly  
19 constrained.

20 Figure 4 compares seasonal gridded mean ammonia concentrations observed by the IASI  
21 instrument with the GEOS-Chem simulation from May 2009 through April 2010. Only  
22 gridboxes with at least 4 observations during a season are shown in order to avoid drawing  
23 conclusions from limited, variable measurements. We first show the number of retrievals  
24 averaged in each gridbox, to demonstrate both the extensive cross-track coverage of IASI, and  
25 the seasonal variability in the number of successful retrievals of ammonia. This is most likely  
26 due to cloud coverage, particularly in the fall and winter. We also see in Figure 4 the high  
27 degree of reliance on the a priori in the retrieval. This is particularly evident when comparing  
28 the native GEOS-Chem simulation with the “retrieved” simulation where the IASI ammonia  
29 averaging kernel and a priori are applied as in equation 1. Both the IASI and GEOS-Chem  
30 retrieved values rarely drop below the a priori column concentration ( $\sim 0.3 \times 10^{16}$  molecules  
31  $\text{cm}^{-2}$ ) and seasonality is reduced, consistent with the reported characteristics of the ammonia  
32 retrievals for the Tropospheric Emission Spectrometer (TES) (Shephard et al., 2011).

1 Furthermore, all the features of the GEOS-Chem ammonia distribution are considerably  
2 damped by application of the averaging kernel.

3 IASI ammonia concentrations peak in the springtime in the Midwest, in contrast with  
4 simulated concentrations which peak in the summertime. However, comparison of the native  
5 and retrieved GEOS-Chem fields suggest that that IASI sensitivity in the Midwest may be  
6 lower in the summer than the springtime, which may contribute to this apparent difference.  
7 The distribution of simulated ammonia agrees reasonably well in the region in summertime,  
8 but the comparison suggests that springtime ammonia emissions are far too low in GEOS-  
9 Chem. This is consistent with Zhang et al. (2012) who find that comparisons with the  
10 MWNH<sub>3</sub> observations support a broadening of the NH<sub>3</sub> emission peak from summer into  
11 spring and fall, with more than a doubling of March and April emissions. Total U.S. ammonia  
12 emissions increase by 18% (see Table 1). Some previous studies also support a springtime  
13 peak in ammonia emissions in the United States (Pinder et al., 2006; Gilliland et al., 2006);  
14 however, optimized ammonia emissions from Henze et al. (2009) peak in the summertime.  
15 These differences in part confirm the challenge of constraining ammonia emissions from wet  
16 deposition or aerosol measurements as done in the preceding studies. The increase in  
17 springtime ammonia concentrations resulting from applying the Zhang et al. (2012)  
18 seasonality in GEOS-Chem is washed out when the IASI averaging kernels are applied and  
19 does not close the gap with the IASI observations. In fact, an extremely large and likely  
20 unrealistic increase in ammonia concentrations (in excess of a factor of 5) would be required  
21 to reconcile the GEOS-Chem simulation with the IASI measurements over the Midwest. As  
22 discussed in Section 2.3 this is due to the artificially low IASI degrees of freedom for signal  
23 and that the averaging kernels do not accurately represent the balance between a priori and  
24 detected information in the retrieval. Thus, for this study, the IASI retrievals are only used  
25 qualitatively. In light of this, we conclude that IASI measurements support the springtime  
26 enhancement of ammonia emissions suggested by Zhang et al., (2012) and include this  
27 increase in the comparisons that follow (referred to as “New NH<sub>3</sub> Seasonality”). Wells et al.  
28 (2012) find a similar springtime underestimate of methanol in the GEOS-Chem simulation  
29 compared to the IASI methanol retrievals, which they attribute to an underestimate of  
30 biogenic emissions from new leaves in mid-latitude ecosystems. Ammonia emissions from  
31 vegetation are negligible (Guenther et al., 2012), thus enhanced springtime emissions are far  
32 more likely associated with agricultural practices, for example earlier fertilizer application in

1 the Midwest, or seasonal changes in cattle feed availability as associated emissions (Hristov et  
2 al., 2011).

3 Figure 4 also indicates that ammonia emissions in California and particularly in the San  
4 Joaquin Valley (SJV) are underestimated in GEOS-Chem. This mainly rural and agricultural  
5 region features some of the largest ammonia emissions in the country (Goebes et al.,  
6 2003;Makar et al., 2009), and regularly reports some of the highest PM loading in the United  
7 States (Chow et al., 1996;Watson et al., 2000), leading to frequent violations of the National  
8 Ambient Air Quality Standards. Clarisse et al. (2010) previously estimated that mean  
9 summertime surface ammonia concentrations in the SJV regionally exceed 15 ppb. Figure 4  
10 shows that California is well-observed by IASI, with the exception of the wintertime, and  
11 while the spatial and seasonal patterns of enhanced ammonia are captured by GEOS-Chem,  
12 IASI concentrations are significantly underestimated from spring through fall. Retrieval  
13 characteristics preclude a quantitative estimate of the associated emissions gap (see previous  
14 discussion); however, an underestimate in ammonia in the region is consistent with the  
15 ammonium nitrate formation underestimate implied by the nitrate underestimate in the region  
16 (Figure 3), as also suggested by Walker et al. (2012). Nowak et al. (2012) report an  
17 underestimate of dairy emissions in the South Coast Air Basin in the NEI-05 emission  
18 inventory which could contribute to the underestimate in California.

19 Figure 5 presents a further evaluation of simulated ammonia, which illustrates some of the  
20 challenges associated with local comparisons and strong regional gradients. We compare  
21 simulated and measured ammonia at four field sites located in some proximity (within 700  
22 km, Figure 1). The model (with “New NH<sub>3</sub> Seasonality” emissions as discussed above)  
23 reproduces ammonia well at the rural site in Wyoming which is removed from local sources.  
24 The Colorado sites represent a strong west to east gradient from the very clean Rocky  
25 Mountain National Park to Brush, CO which is east and often down-wind of one of the largest  
26 inventory of cattle in the United States (Weld County). Observed monthly mean ammonia  
27 concentrations increase more than 20-fold across this gradient, while model concentrations at  
28 most double. While the underestimation of ammonia emissions associated with these  
29 agricultural operations has a limited impact on ammonium nitrate formation in the model  
30 (limited by the nitric acid supply), it implies potentially large underestimates of simulated  
31 regional nitrogen deposition.

1 The qualitative information provided by the IASI instrument suggests that the ammonia  
2 emissions biases may be responsible for two aspects of the GEOS-Chem nitrate simulation  
3 shown in Figure 3: (1) The underestimate of nitrate in California is associated, at least in part,  
4 with an underestimate in ammonia emissions in the region. (2) A springtime underestimate of  
5 ammonia emissions in the Midwest masks some of the bias in nitrate present year-round in  
6 the simulation. Increasing the ammonia emissions in springtime as suggested by Zhang et al.  
7 (2012) increases the nitrate bias seen in Figure 3 (slope increases from 1.04 to 1.77 – see  
8 increase in annual mean nitrate concentrations in Figure 6). Thus, while further validation of  
9 ammonia emission inventories is clearly called for, there is no evidence to suggest that the  
10 excess nitrate levels in GEOS-Chem are associated with biases in emissions.

11

### 12 **4.3 Further exploration of the nitrate bias**

13 Alternate explanations for the nitrate bias in the GEOS-Chem model include errors in nitric  
14 acid formation or deposition. Surface nitric acid concentrations are challenging to evaluate as  
15 a result of the strong vertical gradient associated with surface uptake. Zhang et al. (2012)  
16 make an attempt to account for this by adjusting the lowest model gridbox center (70 m)  
17 simulated concentrations to the 10m CASTNet measurement altitude using an aerodynamic  
18 resistance correction. They report an 18% annual average high bias in the model following  
19 this correction, which they attribute to an overestimation of nitric acid formation via  $N_2O_5$   
20 hydrolysis on ammonium nitrate aerosols. However this is unlikely given that McIntyre and  
21 Evans (2010) show that the sensitivity of the  $NO_x$  budget to a decrease in the uptake  
22 coefficient of  $N_2O_5$  is less than 10% given the current values of the uptake coefficient  
23 assumed in GEOS-Chem. This is confirmed in Figure 6 which shows that nitrate  
24 concentrations decrease by less than 10% when the uptake coefficient of  $N_2O_5$  is reduced by  
25 an order of magnitude in the model.

26 Nitric acid formation could also be promoted by an excessively oxidizing environment.  
27 However, nitrate concentrations are found to be relatively insensitive to modest changes in  
28 OH. A reduction in simulated OH levels by 25% does not impact simulated nitrate levels  
29 (within 5% of baseline concentrations), as a reduction in nitric acid formation is somewhat  
30 compensated by an increase in lifetime. Similarly, ~15% overestimation of the reaction rate of  
31  $NO_2$  oxidation by OH suggested by recent studies (Mollner et al., 2010; Henderson et al.,

1 2012), does not significantly impact nitrate concentrations at the surface over the United  
2 States (within 5% of baseline GEOS-Chem simulated concentrations).

3 An additional sink of nitric acid, not considered in the GEOS-Chem simulation here, is the  
4 uptake of nitric acid on coarse mode dust or sea salt (eg. (Goodman et al., 2000; Abbatt and  
5 Waschewsky, 1998)). Neglecting this effect could lead to a high bias in surface nitric acid,  
6 particularly in the southwest near dust sources, and in coastal regions influenced by coarse  
7 mode sea salt. However, Fairlie et al. (2010) show that including the uptake of nitric acid on  
8 dust in the GEOS-Chem simulation does not eliminate the nitric acid bias in dusty outflow  
9 from Asia. Thus, while this effect may contribute locally to the model overestimate of nitric  
10 acid and fine particulate nitrate, it is unlikely that this can explain the fine nitrate surface bias  
11 through most of the eastern US.

12 Ammonium nitrate formation is favored in cold and humid conditions. GEOS-Chem uses  
13 assimilated meteorology and thus temperature and relative humidity are unlikely to be subject  
14 to large systematic biases. Meteorological parameters are not reported for the IMPROVE sites  
15 shown here, but were made during the field intensives described in Section 2.2. A general  
16 comparison of 2004 simulated values with the temperature and relative humidity detected at  
17 these sites in various years does not reveal any consistent biases. It is therefore highly  
18 unlikely that a strong, consistent, year-round, cold and/or wet bias exists in the model and  
19 could be the cause of excess ammonium nitrate formation. Such a bias would also imply a  
20 corresponding underestimate in nitric acid, which is inconsistent with our simulations and the  
21 results of Zhang et al. (2012). We also verify that surface concentrations of ammonium nitrate  
22 are insensitive to the metastable assumption employed in our implementation of ISORROPIA  
23 II (see Section 3).

24 Errors in deposition of either particle or gas-phase nitrate could contribute to a biased  
25 simulation of nitrate. Zhang et al. (2012) show that annual mean wet deposition of nitrate in  
26 GEOS-Chem is biased slightly high but within 10% of measurements from the National  
27 Atmospheric Deposition Program (NADP) over the continental United States. Dry deposition  
28 of aerosols is size-dependent in the model and any bias in this process would manifest itself in  
29 simulated sulfate as well as nitrate. As the sulfate simulation is relatively unbiased and dry  
30 deposition of particles makes a minor contribution to total nitrogen deposition (Zhang et al.,  
31 2012) we rule this out as a dominant factor in the simulated nitrate overestimate. However,  
32 the dry deposition velocity of nitric acid over various land types is considerably larger and not

1 well constrained. Derived estimates from CASTNet sites across the United States vary from  
2 0.8 to 3.3  $\text{cm s}^{-1}$  (Clarke et al., 1997). Schwede et al. (2011) show that the choice of  
3 deposition models can result in deposition velocities that differ by a factor of 2 to 3, and that  
4 CASTNet estimates of nitric acid deposition velocities are consistently lower than comparable  
5 estimates derived using the CAPMoN network model. Annual mean simulated dry deposition  
6 velocities over the continental United States in GEOS-Chem vary from 0.2 to 3.9  $\text{cm s}^{-1}$ , a  
7 similar range to values reported by CASTNet. Given the poor constraints on this value, we  
8 test the sensitivity of simulated nitrate to the deposition velocity for nitric acid by doubling  
9 this value year-round. Figure 6 shows that particulate nitrate concentrations decrease by less  
10 than 10%, and therefore that uncertainties in deposition velocities cannot reconcile the GEOS-  
11 Chem simulation with the nitrate observations at the IMPROVE sites. Alvarado et al. (2010)  
12 previously showed that nitric acid concentrations measured during the ARCTAS campaign  
13 were overestimated by over a factor of two in GEOS-Chem and invoke insufficient  
14 precipitation scavenging in the Arctic. A good simulation of the wet removal of aerosols over  
15 the continental United States (Fisher et al., 2011) in concert with the high solubility of nitric  
16 acid makes this an unlikely source of the bias here; however, uncertainties in precipitation  
17 distribution and frequency are large and we cannot rule out an underestimate of wet  
18 scavenging as a contributing factor in the nitrate bias.

19 Figure 6 shows that when nitric acid concentrations are artificially decreased to 75% of their  
20 values at each timestep (as an input to the thermodynamic gas-particle partitioning only),  
21 annual mean U.S. surface nitrate concentrations can decrease by up to  $2 \mu\text{g m}^{-3}$ . This decrease  
22 brings the nitrate simulation into near agreement with the IMPROVE measurements (Figure  
23 7), with the exception of California, where the existing bias is exacerbated (see Section 4.1).  
24 Nitrate concentrations remain somewhat high in the Northeast (NMB=0.42 for the Eastern  
25 US), particularly in winter when ammonium nitrate formation is favored. However, overall,  
26 model performance is substantially improved by this forced reduction in nitric acid with NMB  
27 values in the Eastern U.S. considerably lower (all below 0.50) than baseline values shown in  
28 Figure 3. Figure 8 shows how this decreased nitric acid brings the model into agreement with  
29 the ammonia, nitrate and ammonium observations from the Midwest Ammonia Monitoring  
30 Project in 2004. A reduction of nitric acid reduces ammonium nitrate formation and  
31 conversely forces more ammonia into the gas-phase, particularly in the fall and winter.  
32 Ammonium nitrate concentrations may still be overestimated in the simulation, consistent

1 with the Figure 6 comparison with IMPROVE sites, but overall model bias is drastically  
2 reduced.

3 Figure 9 shows that this “updated” simulation with reduced nitric acid also compares well  
4 with the year-round nitrate observations in Wyoming and Colorado. Nitrate at the Loveland  
5 and Brush sites is underestimated in the wintertime with the “updated” simulation, however  
6 Figure 5 suggests that this is associated with an underestimated wintertime supply of  
7 ammonia. Year-round cattle operations in the region likely maintain ammonia emissions in  
8 cooler seasons above the summertime-peaking seasonality currently applied to all  
9 anthropogenic ammonia emissions in the NEI-05 inventory. This calls for a dis-aggregation of  
10 ammonia emissions and an investigation of the seasonality of emissions in various sectors.

11 While we can identify no single process or uncertainty that could result in the current  
12 overestimation of surface nitrate concentrations in the GEOS-Chem simulation, it is clear that  
13 a simple year-round reduction of nitric acid can improve model performance drastically. A  
14 number of processes may potentially contribute to this. First, while we have tested the impact  
15 of oxidant loading and  $\text{N}_2\text{O}_5$  hydrolysis, there may be other unrecognized chemical pathways  
16 for  $\text{NO}_y$  cycling which may reduce nitric acid formation. Second, an underestimate of  
17 deposition of nitric acid could contribute to this bias, however as shown above, this cannot  
18 explain the entire model bias. Third, uptake of  $\text{HNO}_3$  on coarse PM (not treated here) may  
19 reduce both nitric acid and nitrate concentrations, particularly in the dusty southwest. Fourth,  
20 the vertical sub-grid gradient of nitric acid at the surface may induce a similar gradient in  
21 ammonium nitrate formation which has not been accounted for here. Sievering et al.(2001)  
22 find that the vertical gradient in nitrate is weaker than for  $\text{HNO}_3$ , suggesting that  
23 thermodynamic equilibrium may not be maintained through the surface layer. de Brugh et al.  
24 (2012) suggest that not accounting for this effect can mute the simulated diurnal cycle. They  
25 recommend artificially increasing the altitude of the meteorological input parameters in coarse  
26 resolution models to correct for this effect; however, they show that this correction is only  
27 valid in unstable conditions. It is unclear how this would impact the comparison of daily mean  
28 surface concentrations. Additional time-resolved gas-particle vertical profile measurements  
29 through the boundary layer are required to investigate this phenomenon further and develop  
30 an appropriate global correction for coarse resolution models such as GEOS-Chem. We note  
31 that no effort was made to optimize our artificial nitric acid reduction seasonally, and the  
32 uncertainties outlined above may play a role in different seasons, as well as different regions.

1

## 2 **4.4 Application of “updated” simulation**

3 Figure 10 compares this “updated” ( $\text{HNO}_3$  reduced to 75%) simulation with the daily  
4 observations of inorganic PM from the seven focus sites (Section 2.2) as an independent  
5 check on the comparisons discussed in Section 4.3. The timeseries also illustrates the regional  
6 and temporal variability of inorganic PM across the United States. Sites are ordered roughly  
7 west to east. Note that measurements do not correspond to the 2004 year of the simulation for  
8 six of the seven sites, and thus meteorological variability can degrade these comparisons. The  
9 “updated” model simulation reproduces the character of inorganic PM across the US both in  
10 magnitude and variability. Concentrations are highest in the East and contributions from  
11 nitrate are largest in the fall/winter and in the western US. Elevated PM concentrations are  
12 episodic and generally persist for 2-3 days.

13 The seasonal mean simulated gas fraction for the three inorganic classes ( $\text{SO}_x$ ,  $\text{NH}_x$  and total  
14 nitrate) are compared to these same observations in Figure 11. These patterns illustrate the  
15 complex gas-particle partitioning regimes across the United States. This figure particularly  
16 illustrates the spatial variability in gas-particle partitioning and the necessity of using high-  
17 resolution simulations to resolve this behavior and usefully compare with in situ  
18 measurements. We see that sulfate formation is most efficient in the summertime due to  
19 higher oxidant loadings and that the short lifetime of  $\text{SO}_2$  results in gas fraction hot spots near  
20 local sources. GEOS-Chem captures this seasonal  $\text{SO}_x$  partitioning across the United States,  
21 with the exception of the remote Brigantine, NJ site, which itself may experience  
22 predominantly processed emissions as sulfate, but which is located in a gridbox with fresh  
23 emissions.

24 Figure 11 shows that much of the ammonia in the eastern U.S. neutralizes acidity in the  
25 region to form ammonium salts, and thus the N(-III) gas fraction is low. Important source  
26 regions in both California and the Midwest produce excess ammonia which locally remains  
27 predominantly in the gas-phase, particularly in the summertime. The model reproduces the  
28 observed N(-III) partitioning with the exception of the Big Bend site near the Texas-Mexico  
29 border. Observed concentrations of ammonia are very low at this site ( $< 0.4 \mu\text{g m}^{-3}$ ), and are  
30 overestimated by the model by at least a factor of two (likely due to an underestimate in  
31 sulfate, Figure 10). Given the low PM concentrations at the site, this significantly degrades  
32 the gas fraction comparison.

1 Much of the nitric acid in the Eastern U.S. participates in ammonium nitrate formation given  
2 the up-wind source of ammonia from the Midwest. Conversely, much of the Western U.S. is  
3 limited by the ammonia supply. This East-West gradient in the N(V) gas fraction is  
4 reproduced by the model, with the exception of the San Geronio site in California in  
5 springtime, where both complex terrain unresolved by the model, and the ammonia  
6 underestimate discussed in Section 4.2 and seen in Figure 4 likely play a role. We note that  
7 using surface measurements to evaluate the simulation of total nitrate partitioning presumes  
8 that any near-surface gradient is consistent between nitric acid and nitrate.

9 Figure 12 quantifies the nitrogen contribution to inorganic PM mass. In particular we see that  
10 in wintertime nitrogen makes up over a third of inorganic PM mass in the Northern United  
11 States. In all seasons at least 15% of continental inorganic PM mass is nitrogen, and this  
12 fraction will almost certainly grow as drastic further reductions in sulfur emissions expected  
13 in the United States (van Vuuren et al., 2011) are likely to outpace the recent decline in NO<sub>x</sub>  
14 emissions (Pinder et al., 2011). Furthermore, organic nitrogen may contribute significant  
15 additional nitrogen mass to total fine PM (Fry et al., 2009; Rollins et al., 2009).

16

## 17 **5 Conclusions**

18 Model simulations of inorganic PM are typically evaluated by network measurements of  
19 sulfate and nitrate concentrations or wet deposition. Comparison of a 2004 GEOS-Chem  
20 simulation with observations of sulfate and nitrate at IMPROVE sites reveals the following  
21 features: (1) a good simulation of sulfate concentrations year-round with a modest high bias in  
22 the Northeast in the Fall and a modest underestimate in the Southeast in the summer; (2) an  
23 underestimate of nitrate concentrations year-round in California and (3) a large positive bias  
24 in nitrate year-round across the rest of the United States, likely associated with an  
25 overestimate in nitric acid concentrations previously reported by Zhang et al. (2012). IASI  
26 observations confirm that ammonia concentrations are underestimated in California and are  
27 likely the source of the nitrate underestimate in this region. A recent, independent study by  
28 Walker et al. (2012) reaches the same conclusion. A spatially diverse set of full year  
29 observations is required in the region to further characterize the emission discrepancies.  
30 Comparison with IASI also suggests that ammonia concentrations are underestimated in the  
31 springtime with current assumed emission seasonality, however increasing emissions in this  
32 region only exacerbates the nitrate bias.

1 We explore the sensitivity of simulated nitrate to a number of uncertain model parameters  
2 related both to chemistry and deposition but are unable to identify the cause of the model  
3 overestimate. We do find that decreasing nitric acid concentrations uniformly to 75% of  
4 simulated values brings the model into close agreement with the IMPROVE nitrate  
5 measurements, as well as the ammonium and nitrate measured during the Midwest Ammonia  
6 Monitoring Project and the year-round nitrate measured at a suite of sites in Wyoming and  
7 Colorado. Further investigation into the role of sub-grid near-surface processes and the nitric  
8 acid budget are required to resolve this. In particular, tower-based measurements of the  
9 boundary layer vertical profile and fluxes could provide critical insight into this question.  
10 Further investigation of the importance of coarse mode nitrate as a control on nitric acid  
11 concentrations and fine particle nitrate throughout the US is also required.

12 We demonstrate the challenges of reproducing strong ammonia gradients near source regions.  
13 However we also show that the impact of underestimating ammonia near these sources on PM  
14 formation is limited, at least in the near-field. The fate of this excess ammonia and the  
15 prevalence of these underrepresented “hot spot” emissions in the United States requires  
16 further investigation in order to accurately characterize local deposition and ecosystem  
17 response. Furthermore, our full year comparisons for sites in Wyoming and Colorado suggest  
18 that fertilizer and livestock ammonia emissions may exhibit quite different seasonality with  
19 implications for ammonium nitrate formation in wintertime.

20 This study uses a suite of in situ and satellite measurements, in particular focusing on  
21 ammonia, to evaluate our understanding of the inorganic gas-particle system. While we  
22 provide examples of model skill, the complexity of this system remains a challenge to capture  
23 with full fidelity. For example, inclusion of bi-directional treatment of ammonia fluxes may  
24 improve day-to-day variability in the model and the simulation of downwind concentrations  
25 (Cooter et al., 2010). Additional co-located measurements of both gas and particle phase  
26 inorganics are required to further constrain models and refine schemes that can be applied to  
27 accurately characterize both PM formation and nitrogen deposition in the United States.

28

## 29 **Acknowledgements**

30 This work was supported by NOAA (NA12OAR4310064). Measurements at Big Bend NP,  
31 Yosemite NP, San Geronio, Bondville, Brigantine, Great Smoky Mountain NP, Rocky  
32 Mountain NP, Loveland Brush were supported by the National Park Service. Field assistance

1 from D. Day, X. Yu, and B. Ayres is gratefully acknowledged. Measurements at Boulder,  
2 WY were supported by Shell Exploration and Development Company and taken in  
3 collaboration with Air Resource Specialists, Inc. IASI was developed and built under the  
4 responsibility of CNES and flies onboard the MetOp satellite as part of the Eumetsat Polar  
5 system. The IASI L1 data are received through the EUMETCast near real time data  
6 distribution service. LC, PFC and MVD are respectively Postdoctoral Researcher, Research  
7 Associate and FRIA grant holder with F.R.S.-FNRS. CC is grateful to CNES for scientific  
8 collaboration and financial support. The research in Belgium was funded by the BELSPO and  
9 ESA (Prodex arrangements). We acknowledge support from the ECLAIRE project (EU-FP7)  
10 and the “Actions de Recherche Concertées” (Communauté Française de Belgique). Although  
11 this paper has been reviewed by the EPA and approved for publication, it does not necessarily  
12 reflect EPA policies or views.

13

## 1 References

- 2 Aan de Brugh, J. M. J., Henzing, J. S., Schaap, M., Morgan, W. T., van Heerwaarden, C. C.,  
3 Weijers, E. P., Coe, H., and Krol, M. C.: Modelling the partitioning of ammonium nitrate in  
4 the convective boundary layer, *Atmospheric Chemistry and Physics*, 12, 3005-3023,  
5 10.5194/acp-12-3005-2012, 2012.
- 6 Abbatt, J. P. D., and Waschewsky, G. C. G.: Heterogeneous interactions of HOBr, HNO<sub>3</sub>, O-  
7 3, and NO<sub>2</sub> with deliquescent NaCl aerosols at room temperature, *J. Phys. Chem. A*, 102,  
8 3719-3725, 10.1021/jp980932d, 1998.
- 9 Adams, P. J., Seinfeld, J. H., and Koch, D. M.: Global concentrations of tropospheric sulfate,  
10 nitrate, and ammonium aerosol simulated in a general circulation model, *J. Geophys. Res.-*  
11 *Atmos.*, 104, 13791-13823, 1999.
- 12 Alvarado, M. J., Logan, J. A., Mao, J., Apel, E., Riemer, D., Blake, D., Cohen, R. C., Min, K.  
13 E., Perring, A. E., Browne, E. C., Wooldridge, P. J., Diskin, G. S., Sachse, G. W., Fuelberg,  
14 H., Sessions, W. R., Harrigan, D. L., Huey, G., Liao, J., Case-Hanks, A., Jimenez, J. L.,  
15 Cubison, M. J., Vay, S. A., Weinheimer, A. J., Knapp, D. J., Montzka, D. D., Flocke, F. M.,  
16 Pollack, I. B., Wennberg, P. O., Kurten, A., Crouse, J., St Clair, J. M., Wisthaler, A.,  
17 Mikoviny, T., Yantosca, R. M., Carouge, C. C., and Le Sager, P.: Nitrogen oxides and PAN  
18 in plumes from boreal fires during ARCTAS-B and their impact on ozone: an integrated  
19 analysis of aircraft and satellite observations, *Atmospheric Chemistry and Physics*, 10, 9739-  
20 9760, 10.5194/acp-10-9739-2010, 2010.
- 21 Ames, R. B., and Malm, W. C.: Comparison of sulfate and nitrate particle mass  
22 concentrations measured by IMPROVE and the CDN, *Atmos. Environ.*, 35, 905-916, 2001.
- 23 Beem, K. B., Raja, S., Schwandner, F. M., Taylor, C., Lee, T., Sullivan, A. P., Carrico, C. M.,  
24 McMeeking, G. R., Day, D., Levin, E., Hand, J., Kreidenweis, S. M., Schichtel, B., Malm, W.  
25 C., and Collett, J. L.: Deposition of reactive nitrogen during the Rocky Mountain Airborne  
26 Nitrogen and Sulfur (RoMANS) study, *Environ. Pollut.*, 158, 862-872,  
27 10.1016/j.envpol.2009.09.023, 2010.
- 28 Beer, R., Shephard, M. W., Kulawik, S. S., Clough, S. A., Eldering, A., Bowman, K. W.,  
29 Sander, S. P., Fisher, B. M., Payne, V. H., Luo, M. Z., Osterman, G. B., and Worden, J. R.:  
30 First satellite observations of lower tropospheric ammonia and methanol, *Geophysical*  
31 *Research Letters*, 35, 5, L09801  
32 10.1029/2008gl033642, 2008.
- 33 Bessagnet, B., Hodzic, A., Vautard, R., Beekmann, M., Cheinet, S., Honore, C., Liousse, C.,  
34 and Rouil, L.: Aerosol modeling with CHIMERE - preliminary evaluation at the continental  
35 scale, *Atmos. Environ.*, 38, 2803-2817, 10.1016/j.atmosenv.2004.02.034, 2004.
- 36 Blanchard, C. L., and Tanenbaum, S.: Draft Final Technical Memorandum: Analysis of Data  
37 from the Midwest Ammonia Monitoring Project, Envair, Albany, CA, 2005.
- 38 Bouwman, A. F., Lee, D. S., Asman, W. A. H., Dentener, F. J., VanderHoek, K. W., and  
39 Olivier, J. G. J.: A global high-resolution emission inventory for ammonia, *Glob.*  
40 *Biogeochem. Cycle*, 11, 561-587, 1997.
- 41 Chen, D., Wang, Y., McElroy, M. B., He, K., Yantosca, R. M., and Le Sager, P.: Regional  
42 CO pollution in China simulated by the high-resolution nested-grid GEOS-Chem model,  
43 *Atmospheric Chemistry and Physics Discussions*, 5853-5887, 2009.

- 1 Chow, J. C., Watson, J. G., Lu, Z. Q., Lowenthal, D. H., Frazier, C. A., Solomon, P. A.,  
2 Thuillier, R. H., and Magliano, K.: Descriptive analysis of PM(2.5) and PM(10) at regionally  
3 representative locations during SJVAQS/AUSPEX, *Atmos. Environ.*, 30, 2079-2112, 1996.
- 4 Clarisse, L., Clerbaux, C., Dentener, F., Hurtmans, D., and Coheur, P. F.: Global ammonia  
5 distribution derived from infrared satellite observations, *Nature Geoscience*, 2, 479-483,  
6 10.1038/ngeo551, 2009.
- 7 Clarisse, L., Shephard, M. W., Dentener, F., Hurtmans, D., Cady-Pereira, K., Karagulian, F.,  
8 Van Damme, M., Clerbaux, C., and Coheur, P. F.: Satellite monitoring of ammonia: A case  
9 study of the San Joaquin Valley, *J. Geophys. Res.-Atmos.*, 115, 15, D13302  
10 10.1029/2009jd013291, 2010.
- 11 Clarke, J. F., Edgerton, E. S., and Martin, B. E.: Dry Deposition Calculations for the Clean  
12 Air Status and Trends Network, *Atmos. Environ.*, 31, 3367-3678, 1997.
- 13 Clerbaux, C.: Monitoring of atmospheric composition using the thermal infrared IASI/MetOp  
14 sounder, *Atmospheric Chemistry and Physics Discussions*, 8307-8339, 2009.
- 15 Cooter, E. J., Bash, J. O., Walker, J. T., Jones, M. R., and Robarge, W.: Estimation of NH<sub>3</sub>  
16 bi-directional flux from managed agricultural soils, *Atmos. Environ.*, 44, 2107-2115,  
17 10.1016/j.atmosenv.2010.02.044, 2010.
- 18 Dockery, D. W., Pope, C. A., Xu, X. P., Spengler, J. D., Ware, J. H., Fay, M. E., Ferris, B. G.,  
19 and Speizer, F. E.: AN ASSOCIATION BETWEEN AIR-POLLUTION AND MORTALITY  
20 IN 6 UNITED-STATES CITIES, *N. Engl. J. Med.*, 329, 1753-1759, 1993.
- 21 Ellis, R. A., Murphy, J. G., Markovic, M. Z., VandenBoer, T. C., Makar, P. A., Brook, J., and  
22 Mihele, C.: The influence of gas-particle partitioning and surface-atmosphere exchange on  
23 ammonia during BAQS-Met, *Atmospheric Chemistry and Physics*, 11, 133-145, 10.5194/acp-  
24 11-133-2011, 2011.
- 25 Erisman, J. W., Sutton, M. A., Galloway, J., Klimont, Z., and Winiwater, W.: How a century  
26 of ammonia synthesis changed the world, *Nature Geoscience*, 1, 636-639, 10.1038/ngeo325,  
27 2008.
- 28 Fairlie, T. D., Jacob, D. J., Dibb, J. E., Alexander, B., Avery, M. A., van Donkelaar, A., and  
29 Zhang, L.: Impact of mineral dust on nitrate, sulfate, and ozone in transpacific Asian pollution  
30 plumes, *Atmospheric Chemistry and Physics*, 10, 3999-4012, 10.5194/acp-10-3999-2010,  
31 2010.
- 32 Fisher, J. A., Jacob, D. J., Wang, Q., Bahreini, R., Carouge, C. C., Cubison, M. J., Dibb, J. E.,  
33 Diehl, T., Jimenez, J. L., Leibensperger, E. M., Meinders, M. B. J., Pye, H. O. T., Quinn, P.  
34 K., Sharma, S., van Donkelaar, A., and Yantosca, R. M.: Sources, distribution, and acidity of  
35 sulfate-ammonium aerosol in the Arctic in winter-spring, *Atmos. Environ.*, 45, 7301-7318,  
36 2011.
- 37 Fountoukis, C., and Nenes, A.: ISORROPIA II: a computationally efficient thermodynamic  
38 equilibrium model for K<sup>+</sup>-Ca<sup>2+</sup>-Mg<sup>2+</sup>-NH<sub>4</sub><sup>(+)</sup>-Na<sup>+</sup>-SO<sub>4</sub><sup>2-</sup>-NO<sub>3</sub><sup>-</sup>-Cl<sup>-</sup>-H<sub>2</sub>O aerosols,  
39 *Atmospheric Chemistry and Physics*, 7, 4639-4659, 2007.
- 40 Fry, J. L., Kiendler-Scharr, A., Rollins, A. W., Wooldridge, P. J., Brown, S. S., Fuchs, H.,  
41 Dube, W. P., Mensah, A., dal Maso, M., Tillmann, R., Dorn, H.-P., Brauers, T., and Cohen,  
42 R. C.: Organic nitrate and secondary organic aerosol yield from NO<sub>3</sub> oxidation of beta-pinene  
43 evaluated using a gas-phase kinetics/aerosol partitioning model, *Atmospheric Chemistry and  
44 Physics*, 9, 1431-1449, 2009.

1 Gilliland, A. B., Appel, K. W., Pinder, R. W., and Dennis, R. L.: Seasonal NH<sub>3</sub> emissions for  
2 the continental United States: Inverse model estimation and evaluation, 2006,  
3 ISI:000240175300015, 4986-4998,

4 Goebes, M. D., Strader, R., and Davidson, C.: An ammonia emission inventory for fertilizer  
5 application in the United States, *Atmos. Environ.*, 37, 2539-2550, 10.1016/s1352-  
6 2310(03)00129-8, 2003.

7 Goodman, A. L., Underwood, G. M., and Grassian, V. H.: A laboratory study of the  
8 heterogeneous reaction of nitric acid on calcium carbonate particles, *J. Geophys. Res.-Atmos.*,  
9 105, 29053-29064, 10.1029/2000jd900396, 2000.

10 Guenther, A. B., Jiang, X., Heald, C. L., Sakulyanontvittaya, T., Duhl, T., Emmons, L. K.,  
11 and Wang, X.: The Model of Emissions of Gases and Aerosols from Nature version 2.1  
12 (MEGAN 2.1): an extended and updated framework for modeling biogenic emissions,  
13 *Geoscientific Model Development Discussions*, 5, 1503-1560, 2012.

14 Henderson, B. H., Pinder, R. W., Crooks, J., Cohen, R. C., Carlton, A. G., Pye, H. O. T., and  
15 Vizuete, W.: Combining Bayesian methods and aircraft observations to constrain the HO  
16 center dot+NO<sub>2</sub> reaction rate, *Atmospheric Chemistry and Physics*, 12, 653-667,  
17 10.5194/acp-12-653-2012, 2012.

18 Henze, D. K., Seinfeld, J. H., and Shindell, D. T.: Inverse modeling and mapping US air  
19 quality influences of inorganic PM<sub>2.5</sub> precursor emissions using the adjoint of GEOS-Chem,  
20 *Atmospheric Chemistry and Physics*, 9, 5877-5903, 2009.

21 Hristov, A. N., Hanigan, M., Cole, A., Todd, R., McAllister, T. A., Ndegwa, P. M., and Rotz,  
22 A.: Review: Ammonia emissions from dairy farms and beef feedlots, *Can. J. Anim. Sci.*, 91,  
23 1-35, 10.4141/cjas10034, 2011.

24 Hurtmans, D., Coheur, P.-F., Wespes, C., Clarisse, L., Scarf, O., Clerbaux, C., Hadji-Lazaro,  
25 J., George, M., and Turquety, S.: FORLI radiative transfer and retrieval code for IASI, *J.*  
26 *Quant. Spectros. Radiat. Transfer*, 113, 1391-1408, 2012.

27 Koracin, D., and Berkowicz, R.: NOCTURNAL BOUNDARY-LAYER HEIGHT -  
28 OBSERVATIONS BY ACOUSTIC SOUNDERS AND PREDICTIONS IN TERMS OF  
29 SURFACE-LAYER PARAMETERS, *Bound.-Layer Meteor.*, 43, 65-83,  
30 10.1007/bf00153969, 1988.

31 Lamsal, L. N., Martin, R. V., Padmanabhan, A., van Donkelaar, A., Zhang, Q., Sioris, C. E.,  
32 Chance, K., Kurosu, T. P., and Newchurch, M. J.: Application of satellite observations for  
33 timely updates to global anthropogenic NO(x) emission inventories, *Geophys. Res. Lett.*, 38,  
34 5, L05810  
35 10.1029/2010gl046476, 2011.

36 Lee, T., Kreidenweis, S. M., and Collett Jr., J. L.: Aerosol Ion Characteristics during the Big  
37 Bend Regional Aerosol and Visibility Observational Study, *Journal of Air & Waste*  
38 *Management Association*, 54, 585-592, 2004.

39 Lee, T., Yu, X.-Y., Ayres, B., Kreidenweis, S. M., Malm, W. C., and Collett Jr., J. L.:  
40 Observation of fine and coarse particle nitrate at several rural locations in the United States,  
41 *Atmospheric Environment*, 42, 2720-2732, 2008a.

42 Lee, T., Yu, X. Y., Kreidenweis, S. M., Malm, W. C., and Collett, J. L.: Semi-continuous  
43 measurement of PM<sub>2.5</sub> ionic composition at several rural locations in the United States,  
44 *Atmos. Environ.*, 42, 6655-6669, 10.1016/j.atmosenv.2008.04.023, 2008b.

- 1 Lin, J. T., and McElroy, M. B.: Impacts of boundary layer mixing on pollutant vertical  
2 profiles in the lower troposphere: Implications to satellite remote sensing, *Atmos. Environ.*,  
3 44, 1726-1739, 10.1016/j.atmosenv.2010.02.009, 2010.
- 4 Liu, H. Y., Jacob, D. J., Bey, I., and Yantosca, R. M.: Constraints from Pb-210 and Be-7 on  
5 wet deposition and transport in a global three-dimensional chemical tracer model driven by  
6 assimilated meteorological fields, *J. Geophys. Res.-Atmos.*, 106, 12109-12128, 2001.
- 7 Makar, P. A., Moran, M. D., Zheng, Q., Cousineau, S., Sassi, M., Duhamel, A., Besner, M.,  
8 Davignon, D., Crevier, L. P., and Bouchet, V. S.: Modelling the impacts of ammonia  
9 emissions reductions on North American air quality, *Atmospheric Chemistry and Physics*, 9,  
10 7183-7212, 2009.
- 11 Malm, W. C., Sisler, J. F., Huffman, D., Eldred, R. A., and Cahill, T. A.: Spatial and seasonal  
12 trends in particle concentration and optical extinction in the United States, *J. Geophys. Res.-*  
13 *Atmos.*, 99, 1347-1370, 1994.
- 14 Malm, W. C., Schichtel, B. A., Pitchford, M. L., Ashbaugh, L. L., and Eldred, R. A.: Spatial  
15 and monthly trends in speciated fine particle concentration in the United States, *J. Geophys.*  
16 *Res.-Atmos.*, 109, 33, D03306  
17 10.1029/2003jd003739, 2004.
- 18 Martin, R. V., Sioris, C. E., Chance, K., Ryerson, T. B., Bertram, T. H., Wooldridge, P. J.,  
19 Cohen, R. C., Neuman, J. A., Swanson, A., and Flocke, F. M.: Evaluation of space-based  
20 constraints on global nitrogen oxide emissions with regional aircraft measurements over and  
21 downwind of eastern North America, *J. Geophys. Res.-Atmos.*, 111, 15, D15308  
22 10.1029/2005jd006680, 2006.
- 23 McIntyre, H. L., and Evans, M. J.: Sensitivity of a global model to the uptake of N<sub>2</sub>O<sub>5</sub> by  
24 tropospheric aerosol, *Atmospheric Chemistry and Physics*, 10, 7409-7414, doi:10.5194/acp-  
25 10-7409-2010, 2010.
- 26 Mollner, A. K., Valluvadasan, S., Feng, L., Sprague, M. K., Okumura, M., Milligan, D. B.,  
27 Bloss, W. J., Sander, S. P., Martien, P. T., Harley, R. A., McCoy, A. B., and Carter, W. P. L.:  
28 Rate of Gas Phase Association of Hydroxyl Radical and Nitrogen Dioxide, *Science*, 330, 646-  
29 649, 10.1126/science.1193030, 2010.
- 30 NARSTO: Particulate Matter Science for Policy Makers: A NARSTO Assessment,  
31 Cambridge, England, 2004.
- 32 Nowak, J. B., Huey, L. G., Russell, A. G., Tian, D., Neuman, J. A., Orsini, D., Sjostedt, S. J.,  
33 Sullivan, A. P., Tanner, D. J., Weber, R. J., Nenes, A., Edgerton, E., and Fehsenfeld, F. C.:  
34 Analysis of urban gas phase ammonia measurements from the 2002 Atlanta Aerosol  
35 Nucleation and Real-Time Characterization Experiment (ANARChE), *J. Geophys. Res.-*  
36 *Atmos.*, 111, 14, D17308  
37 10.1029/2006jd007113, 2006.
- 38 Nowak, J. B., Neuman, A. J., Bahreini, R., Brock, C. A., Middlebrook, A. M., Wollny, A. G.,  
39 Holloway, J. S., Peischl, J., Ryerson, T. B., and Fehsenfeld, F. C.: Airborne observations of  
40 ammonia and ammonium nitrate formation over Houston, TX, *J. Geophys. Res.*,  
41 doi:10.1029/2010JD014195, 2010.
- 42 Nowak, J. B., Neuman, J. A., Bahreini, R., Middlebrook, A. M., Holloway, J. S., McKeen, S.  
43 A., Parish, D. D., Ryerson, T. B., and Trainer, M.: Ammonia sources in the California South

1 Coast Air Basin and their impact on ammonium nitrate formation, *Geophys. Res. Lett.*, 39,  
2 doi:10.1029/2012GL051197, 2012.

3 Park, R. J., Jacob, D. J., Field, B. D., Yantosca, R. M., and Chin, M.: Natural and  
4 transboundary pollution influences on sulfate-nitrate-ammonium aerosols in the United  
5 States: Implications for policy, *J. Geophys. Res.-Atmos.*, 109, D15204,  
6 doi:10.1029/2003JD004473, 2004.

7 Pinder, R. W., Adams, P. J., Pandis, S. N., and Gilliland, A. B.: Temporally resolved  
8 ammonia emission inventories: Current estimates, evaluation tools, and measurement needs,  
9 *J. Geophys. Res.-Atmos.*, 111, 14, D16310  
10 10.1029/2005jd006603, 2006.

11 Pinder, R. W., Adams, P. J., and Pandis, S. N.: Ammonia emission controls as a cost-effective  
12 strategy for reducing atmospheric particulate matter in the eastern United States, *Environ. Sci.*  
13 *Technol.*, 41, 380-386, 10.1021/es060379a, 2007.

14 Pinder, R. W., Gilliland, A. B., and Dennis, R. L.: Environmental impact of atmospheric NH<sub>3</sub>  
15 emissions under present and future conditions in the eastern United States, *Geophys. Res.*  
16 *Lett.*, 35, 6, L12808  
17 10.1029/2008gl033732, 2008.

18 Pinder, R. W., Appel, K. W., and Dennis, R. L.: Trends in atmospheric reactive nitrogen for  
19 the Eastern United States, *Environ. Pollut.*, 159, 3138-3141, 10.1016/j.envpol.2011.04.042,  
20 2011.

21 Pope, C. A., Ezzati, M., and Dockery, D. W.: Fine-Particulate Air Pollution and Life  
22 Expectancy in the United States, *N. Engl. J. Med.*, 360, 376-386, 2009.

23 Pye, H. O. T., Liao, H., Wu, S., Mickley, L. J., Jacob, D. J., Henze, D. K., and Seinfeld, J. H.:  
24 Effect of changes in climate and emissions on future sulfate-nitrate-ammonium aerosol levels  
25 in the United States, *J. Geophys. Res.-Atmos.*, 114, 18, D01205  
26 10.1029/2008jd010701, 2009.

27 Rodgers, C. D.: *Inverse Methods for Atmospheric Sounding: Theory and Practice*, World  
28 Scientific Publishing Co., Singapore, 238 pp., 2000.

29 Rollins, A. W., Kiendler-Scharr, A., Fry, J. L., Brauers, T., Brown, S. S., Dorn, H.-P., Dube,  
30 W. P., Fuchs, H., Mensah, A., Mentel, T. F., Rohrer, F., Tillmann, R., WEgener, R.,  
31 Wooldridge, P. J., and Cohen, R. C.: Isoprene oxidation by nitrate radical: alkyl nitrate and  
32 secondary organic aerosol yields, *Atmospheric Chemistry and Physics*, 9, 6685-6703, 2009.

33 Schwede, D., Zhang, L. M., Vet, R., and Lear, G.: An intercomparison of the deposition  
34 models used in the CASTNET and CAPMoN networks, *Atmos. Environ.*, 45, 1337-1346,  
35 10.1016/j.atmosenv.2010.11.050, 2011.

36 Shephard, M. W., Cady-Pereira, K. E., Luo, M., Henze, D. K., Pinder, R. W., Walker, J. T.,  
37 Rinsland, C. P., Bash, J. O., Zhu, L., Payne, V. H., and Clarisse, L.: TES ammonia retrieval  
38 strategy and global observations of the spatial and seasonal variability of ammonia  
39 *Atmospheric Chemistry and Physics*, 11, 10743-10763, 10.5194/acp-11-10743-2011, 2011.

40 Sievering, H., Kelly, T., McConville, G., Seibold, C., and Turpinseed, A.: Nitric acid dry  
41 deposition to conifer forests: Niwot Ridge spruce-fir-pine study, *Atmos. Environ.*, 35, 3851-  
42 3859, 2001.

1 Sweet, C., Caughey, M., and Gay, D.: Midwest Ammonia Monitoring Project: Summary for  
2 October 2003 through November 2004, Illinois State Water Survey, Champaign, IL, 47, 2005.

3 van der Werf, G. R., Randerson, J. T., Giglio, L., Collatz, G. J., Kasibhatla, P. S., and  
4 Arellano, A. F.: Interannual variability in global biomass burning emissions from 1997 to  
5 2004, *Atmospheric Chemistry and Physics*, 6, 3423-3441, 2006.

6 van Donkelaar, A., Martin, R. V., Leaitch, W. R., Macdonald, A. M., Walker, T. W., Streets,  
7 D. G., Zhang, Q., Dunlea, E. J., Jimenez, J. L., Dibb, J. E., Huey, L. G., Weber, R., and  
8 Andreae, M. O.: Analysis of aircraft and satellite measurements from the Intercontinental  
9 Chemical Transport Experiment (INTEX-B) to quantify long-range transport of East Asian  
10 sulfur to Canada, *Atmospheric Chemistry and Physics*, 8, 2999-3014, 2008.

11 van Vuuren, D. P., Edmonds, J., Kainuma, M., Riahi, K., Thomson, A., Hibbard, K., Hurtt, G.  
12 C., Kram, T., Krey, V., Lamarque, J. F., Masui, T., Meinshausen, M., Nakicenovic, N., Smith,  
13 S. J., and Rose, S. K.: The representative concentration pathways: an overview, *Clim.*  
14 *Change*, 109, 5-31, 10.1007/s10584-011-0148-z, 2011.

15 von Bobruzki, K., Braban, C. F., Famulari, D., Jones, S. K., Blackall, T., Smith, T. E. L.,  
16 Blom, M., Coe, H., Gallagher, M., Ghalaieny, M., McGillen, M. R., Percival, C. J.,  
17 Whitehead, J. D., Ellis, R., Murphy, J., Mohacsi, A., Pogany, A., Junninen, H., Rantanen, S.,  
18 Sutton, M. A., and Nemitz, E.: Field inter-comparison of eleven atmospheric ammonia  
19 measurement techniques, *Atmospheric Measurement Techniques*, 3, 91-112, 2010.

20 Walker, J. M., Seinfeld, J. H., Clarisse, L., Coheur, P.-F., Clerbaux, C., and Van Damme, M.:  
21 Simulation of nitrate, sulfate, and ammonium aerosols over the United States, *Atmospheric*  
22 *Chemistry and Physics Discussions*, submitted, 2012.

23 Wang, J., Hoffmann, A. A., Park, R. J., Jacob, D. J., and Martin, S. T.: Global distribution of  
24 solid and aqueous sulfate aerosols: Effect of the hysteresis of particle phase transitions, *J.*  
25 *Geophys. Res.-Atmos.*, 113, 11, D11206  
26 10.1029/2007jd009367, 2008.

27 Watson, J. G., Chow, J. C., Bowen, J. L., Lowenthal, D. H., Hering, S., Ouchida, P., and  
28 Oslund, W.: Air quality measurements from the Fresno Supersite, *J. Air Waste Manage.*  
29 *Assoc.*, 50, 1321-1334, 2000.

30 Wells, K. C., Millet, D. B., Hu, L., Cady-Pereira, K. E., Xiao, Y., Shephard, M. W., Clerbaux,  
31 C. L., Clarisse, L., Coheur, P.-F., Apel, E. C., De Gouw, J., Warneke, C., Singh, H. B.,  
32 Goldstein, A. H., and Sive, B. C.: Tropospheric methanol observations from space: retrieval  
33 evaluation and constraints on the seasonality of biogenic emissions, *Atmospheric Chemistry*  
34 *and Physics Discussions*, 12, 3941-3982, 2012.

35 Wesely, M. L.: Parameterization of surface resistances to gaseous dry deposition in regional  
36 scale numerical models, *Atmos. Environ.*, 23, 1293-1304, 1989.

37 Yu, S. C., Dennis, R., Roselle, S., Nenes, A., Walker, J., Eder, B., Schere, K., Swall, J., and  
38 Robarge, W.: An assessment of the ability of three-dimensional air quality models with  
39 current thermodynamic equilibrium models to predict aerosol NO<sub>3</sub>, *J. Geophys. Res.-Atmos.*,  
40 110, 25, D07s13  
41 10.1029/2004jd004718, 2005a.

42 Yu, X.-Y., Lee, T., Ayres, B., Kreidenweis, S. M., and Collett Jr, J. L.: Particulate nitrate  
43 measurement using nylon filters, *Journal of the Air & Waste Management Association*, 55,  
44 1100 - 1110, 2005b.

1 Yu, X. Y., Lee, T., Ayres, B., Kreidenweis, S. M., Malm, W., and Collett, J. L.: Loss of fine  
2 particle ammonium from denuded nylon filters, *Atmos. Environ.*, 40, 4797-4807,  
3 10.1016/j.atmosenv.2006.03.061, 2006.

4 Zhang, L., Jacob, D. J., Knipping, E. M., Kumar, N., Munger, J. W., Carouge, C. C., van  
5 Donkelaar, A., Wang, Y. X., and Chen, D.: Nitrogen deposition to the United States:  
6 distribution, sources and processes, *Atmospheric Chemistry and Physics*, 12, 4539-4554,  
7 10.5194/acp-12-4539-2012, 2012.

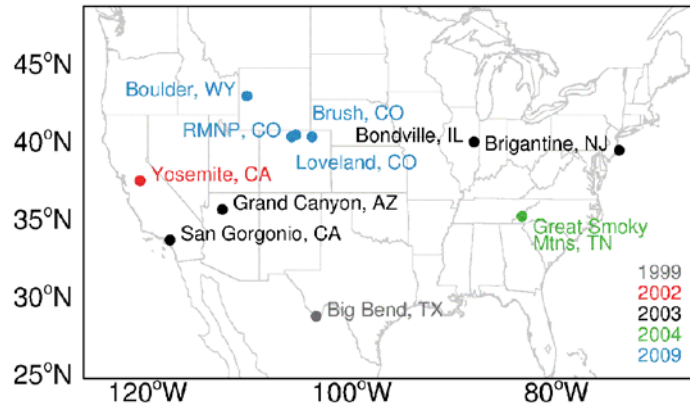
8

9

1 Table 1. Continental U.S. emissions for 2004. Ammonia emissions with “new  
 2 seasonality” shown in brackets (see Section 4.2)

Species	Emission
<b>Ammonia (NH<sub>3</sub>)</b>	<b>2.8 (3.3) TgNyr<sup>-1</sup></b>
Anthropogenic	2.0 (2.5)
Biofuel	0.2
Biomass Burning	0.002
Natural	0.6
<b>Sulfur Oxides (SO<sub>x</sub>)</b>	<b>6.8 TgSyr<sup>-1</sup></b>
Anthropogenic	6.7
Biofuel	0.001
Aircraft	0.01
Biomass Burning	0.09
Volcanic	0.02
<b>Nitrogen Oxides (NO<sub>x</sub>)</b>	<b>6.8 TgNyr<sup>-1</sup></b>
Anthropogenic	5.5
Biofuel	0.01
Aircraft	0.2
Fertilizer	0.09
Biomass Burning	0.03
Lightning	0.7
Soil	0.4

3

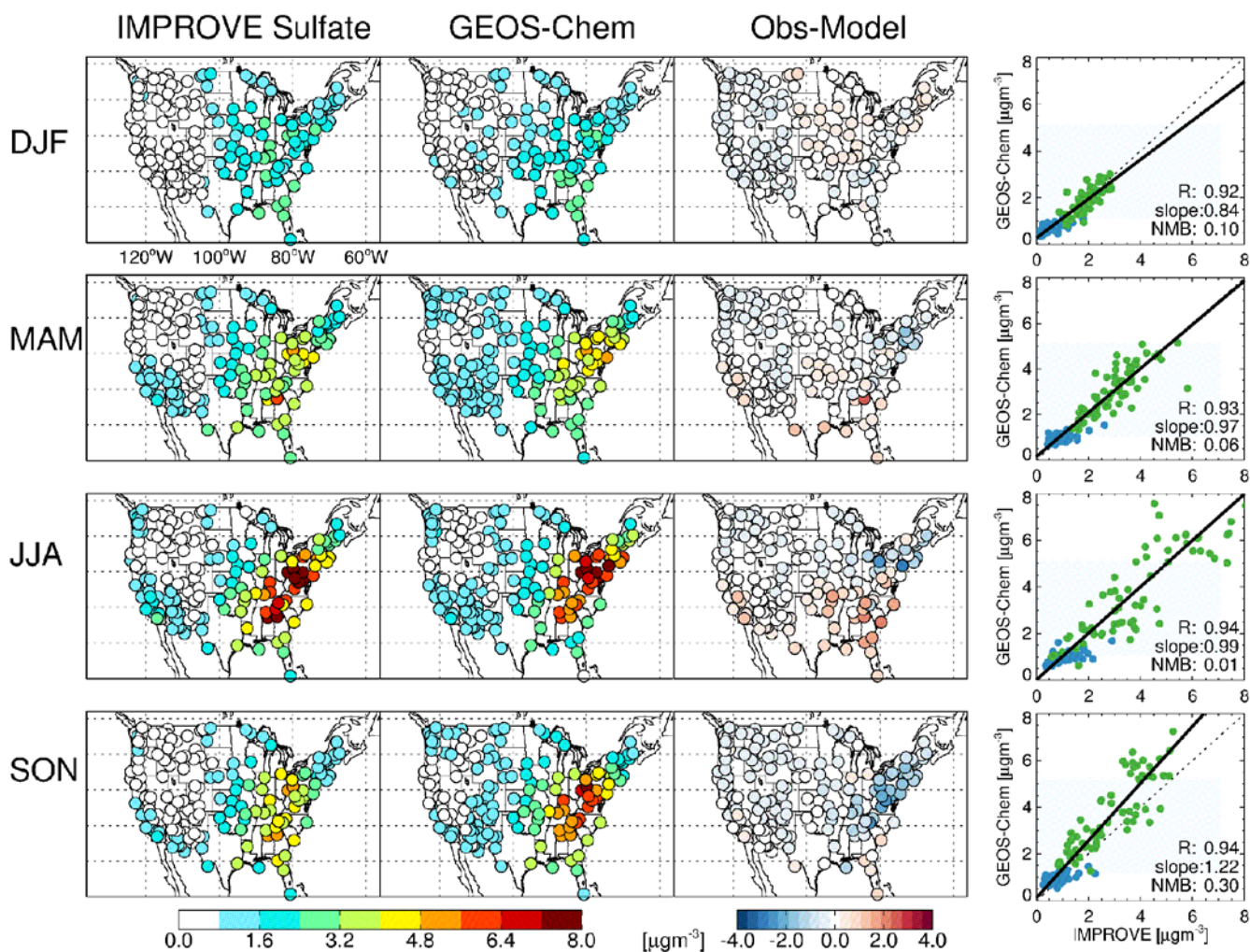


1

2 Figure 1: Surface measurement site locations, colored by year of measurement.

3

4



1

2 Figure 2: Sulfate mean seasonal surface concentrations measured, simulated with GEOS-  
 3 Chem (baseline simulation), and the difference at IMPROVE sites in 2004. Scatterplot of  
 4 seasonal means also shown with reduced-major-axis regression fit (solid black line).

5 Correlation coefficient (R), slope and normalized mean bias (NMB) shown in inset. Sites  
 6 located west of 100°W shown in blue, sites east of this longitude shown in green (longitude  
 7 labels given in top panel for reference).

8

9

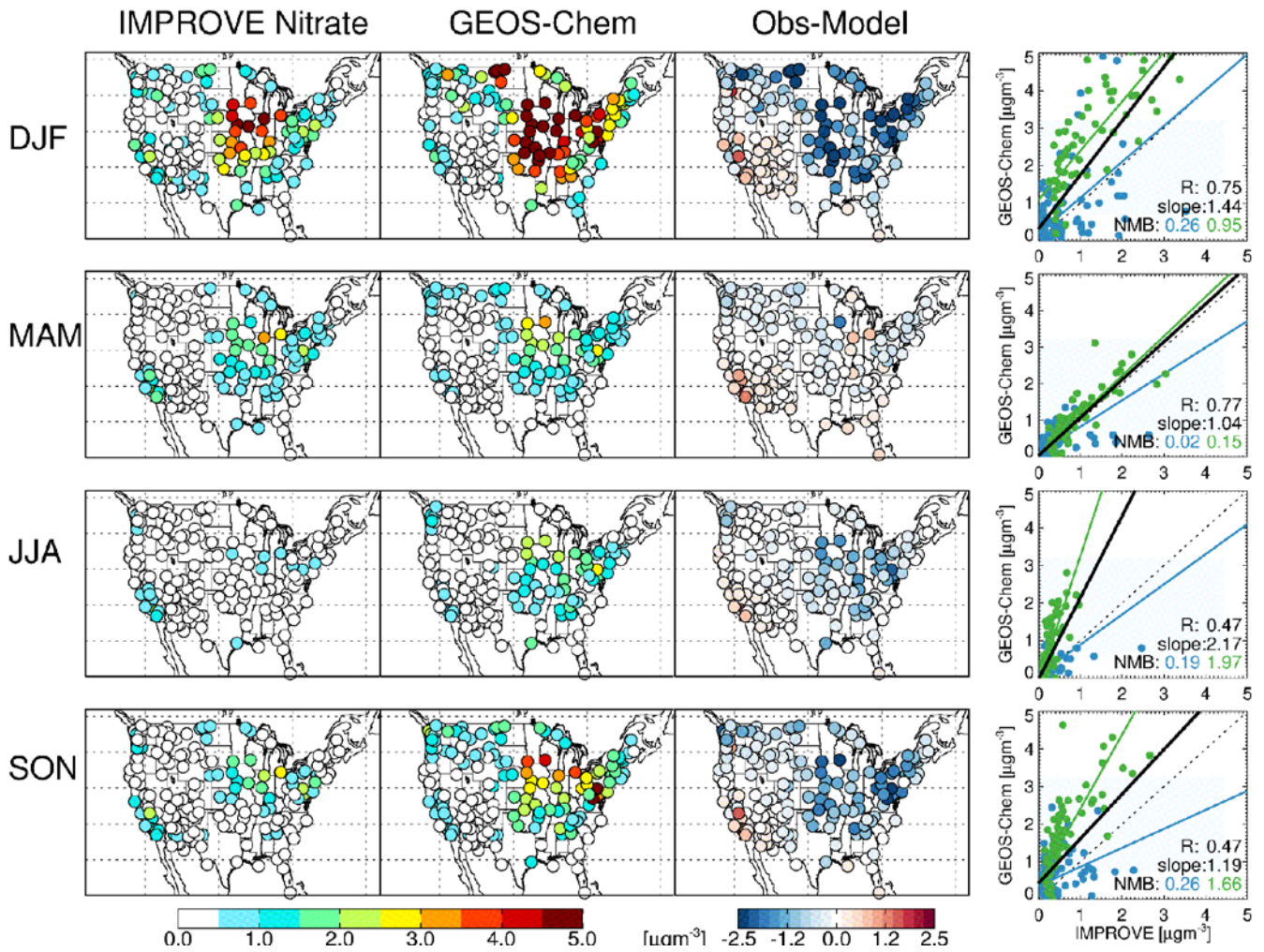
10

11

12

13

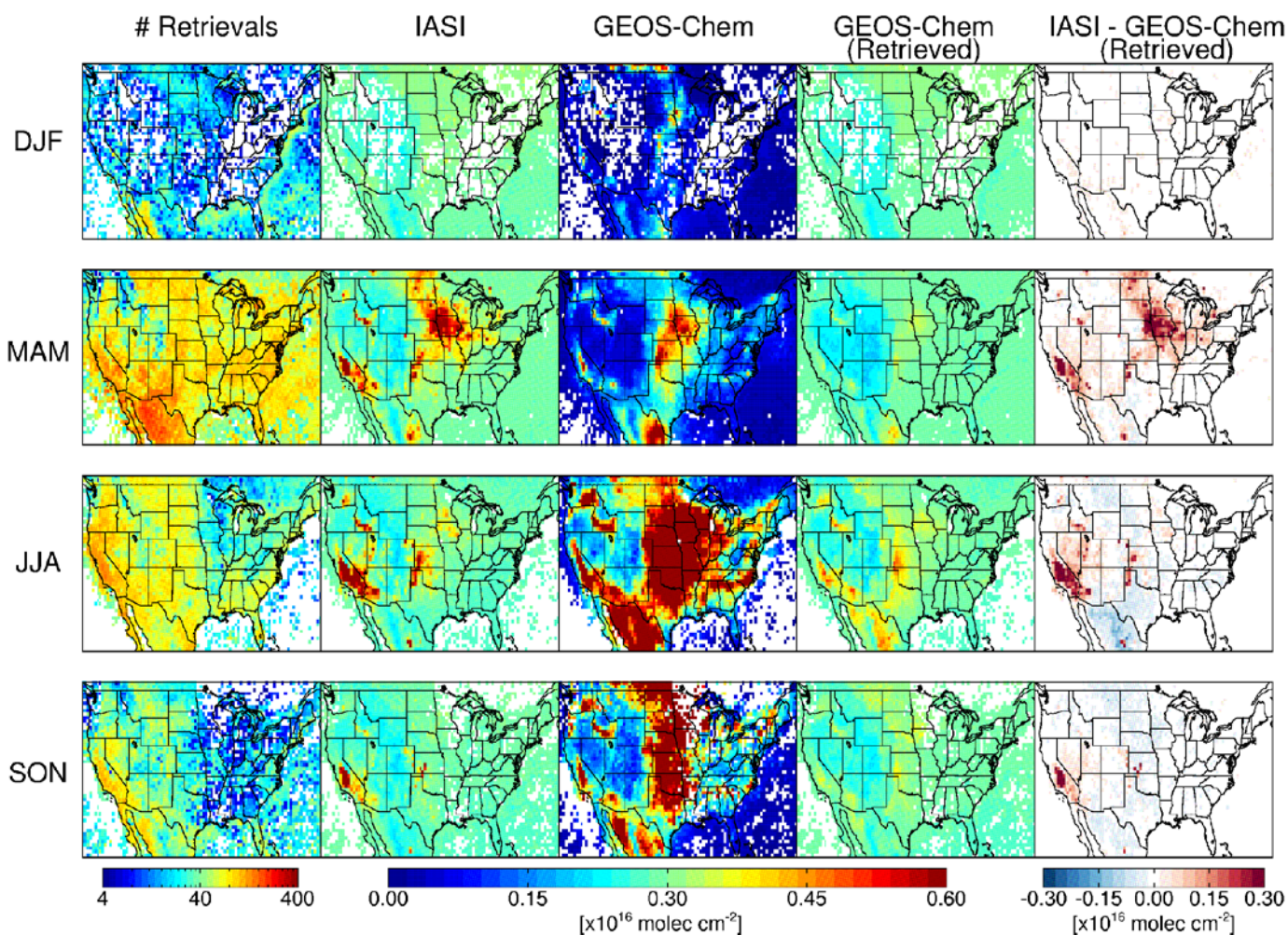
14



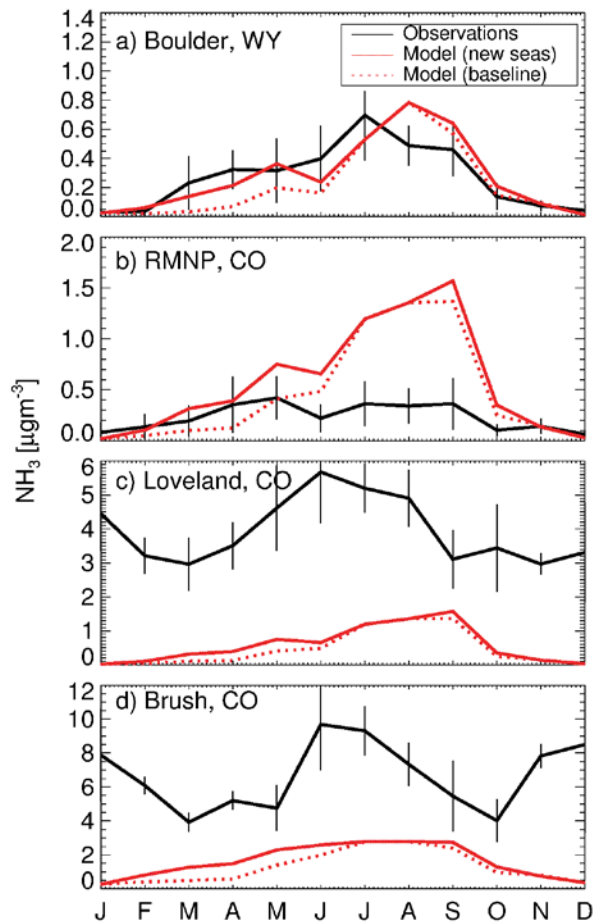
1

2 Figure 3: Nitrate mean seasonal surface concentrations measured, simulated with GEOS-  
 3 Chem (baseline simulation), and the difference at IMPROVE sites in 2004. Scatterplot of  
 4 seasonal means also shown with reduced-major-axis regression fit (solid black line). Sites  
 5 located west of  $100^{\circ}\text{W}$  shown in blue, sites east of this longitude shown in green, with  
 6 reduced-major-axis regression fits for each shown separately as solid lines. Correlation  
 7 coefficient (R), slope and normalized mean bias (NMB) for east and west region shown in  
 8 inset.

9



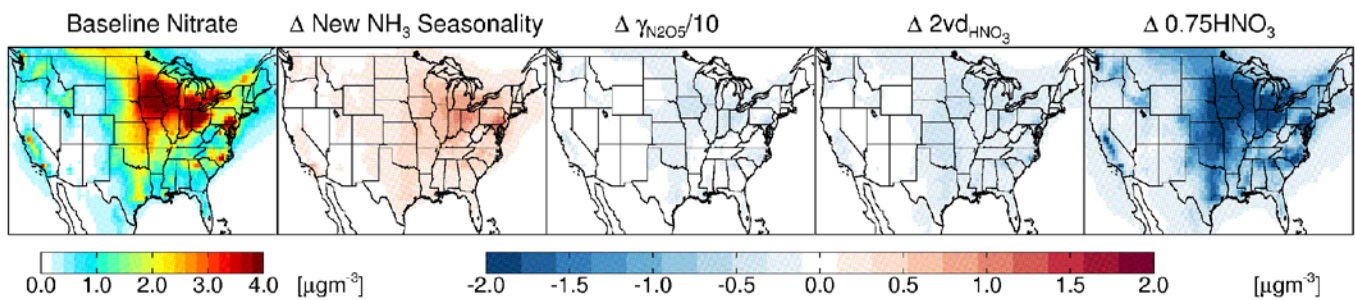
1  
 2 Figure 4: Comparison of atmospheric ammonia column concentrations observed by IASI and  
 3 simulated with the baseline GEOS-Chem model over the United States from May 2009  
 4 through April 2010. The IASI retrieval averaging kernel and a priori have been applied to the  
 5 GEOS-Chem simulation as in equation 1 (4<sup>th</sup> column) for quantitative comparison with the  
 6 satellite observations. Gridded model and observations only shown in gridboxes with 4 or  
 7 more retrievals per season. Color scales are saturated at respective values.



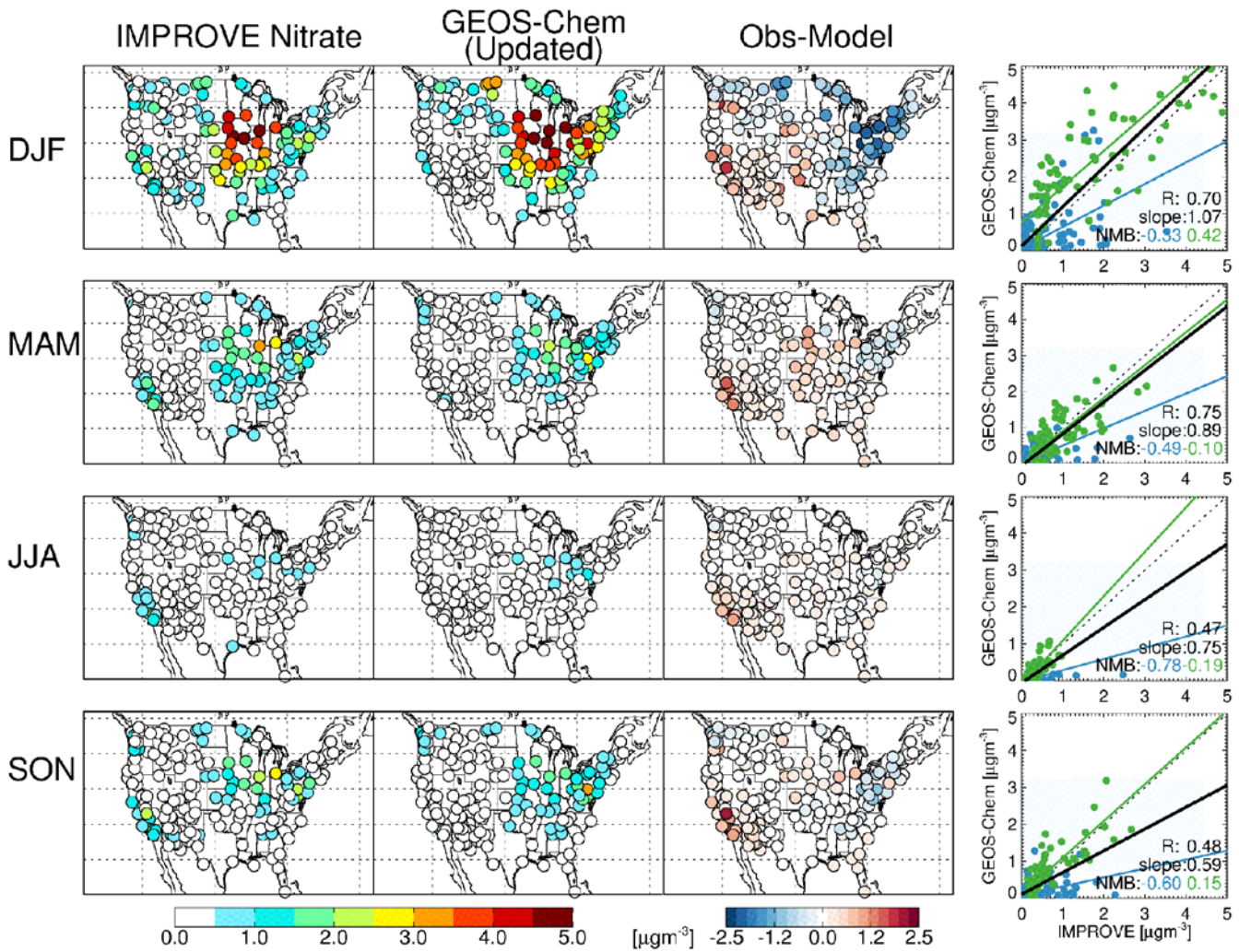
1

2 Figure 5: Timeseries of year-long monthly mean ammonia concentrations measured (black)  
 3 and simulated (red) in 2009 at 4 sites (from west to east): a) Boulder, WY, b) Rocky  
 4 Mountain National Park, CO, c) Loveland, CO and d) Brush, CO. Both the baseline  
 5 simulation (dotted) and simulation with updated ammonia emissions seasonality (solid) are  
 6 shown. Standard deviations of the individual observations averaged for each month are  
 7 shown as error bars.

8

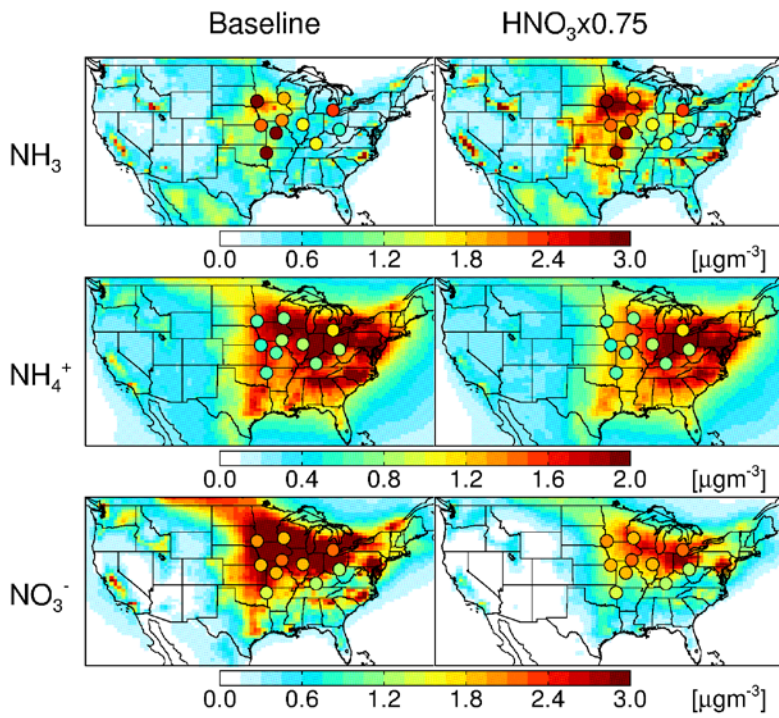


2 Figure 6: Annual mean simulated surface nitrate (left) and the difference from this baseline  
3 (labeled as  $\Delta$ ) for four sensitivity simulations. The four sensitivity simulations are as follows  
4 from left to right: (1) The increase in springtime ammonia emissions, (2) the decrease in the  
5 uptake coefficient of  $\text{N}_2\text{O}_5$  by a factor of 10, (3) a doubling of the dry deposition velocity for  
6 nitric acid and (4) a reduction of nitric acid concentrations to 75% of baseline values.



1 Figure 7: Nitrate mean seasonal surface concentrations measured, simulated with GEOS-  
 2 Chem (updated simulation where  $\text{HNO}_3$  is reduced to 75% of baseline concentrations), and  
 3 the difference at IMPROVE sites in 2004. Scatterplot of seasonal means also shown with  
 4 reduced-major-axis regression fit (solid black line). Sites located west of  $100^\circ\text{W}$  shown in  
 5 blue, sites east of this longitude shown in green, with reduced-major-axis regression fits for  
 6 each shown separately as solid lines. Correlation coefficient (R), slope and normalized mean  
 7 bias (NMB) for east and west region shown in inset. Compare to Figure 3.

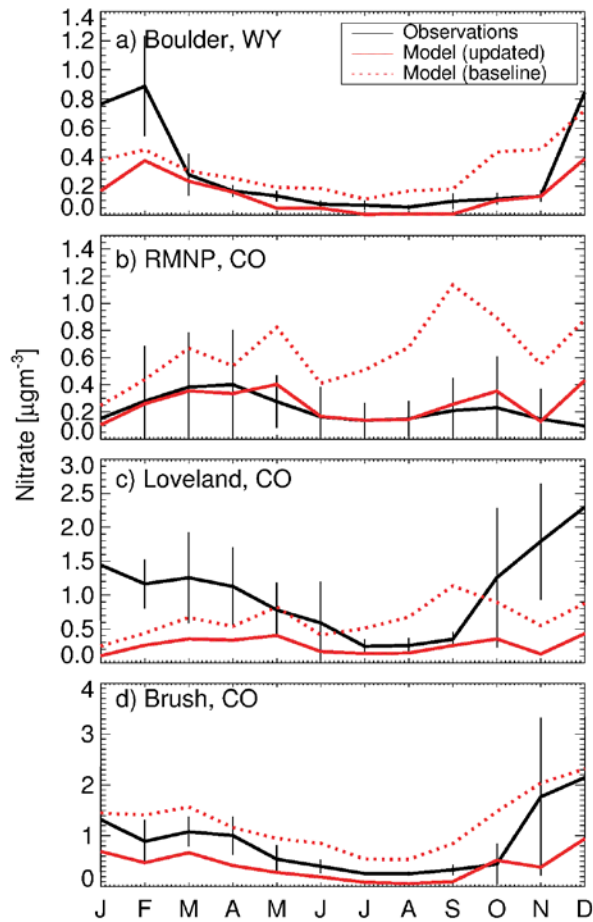
8



1

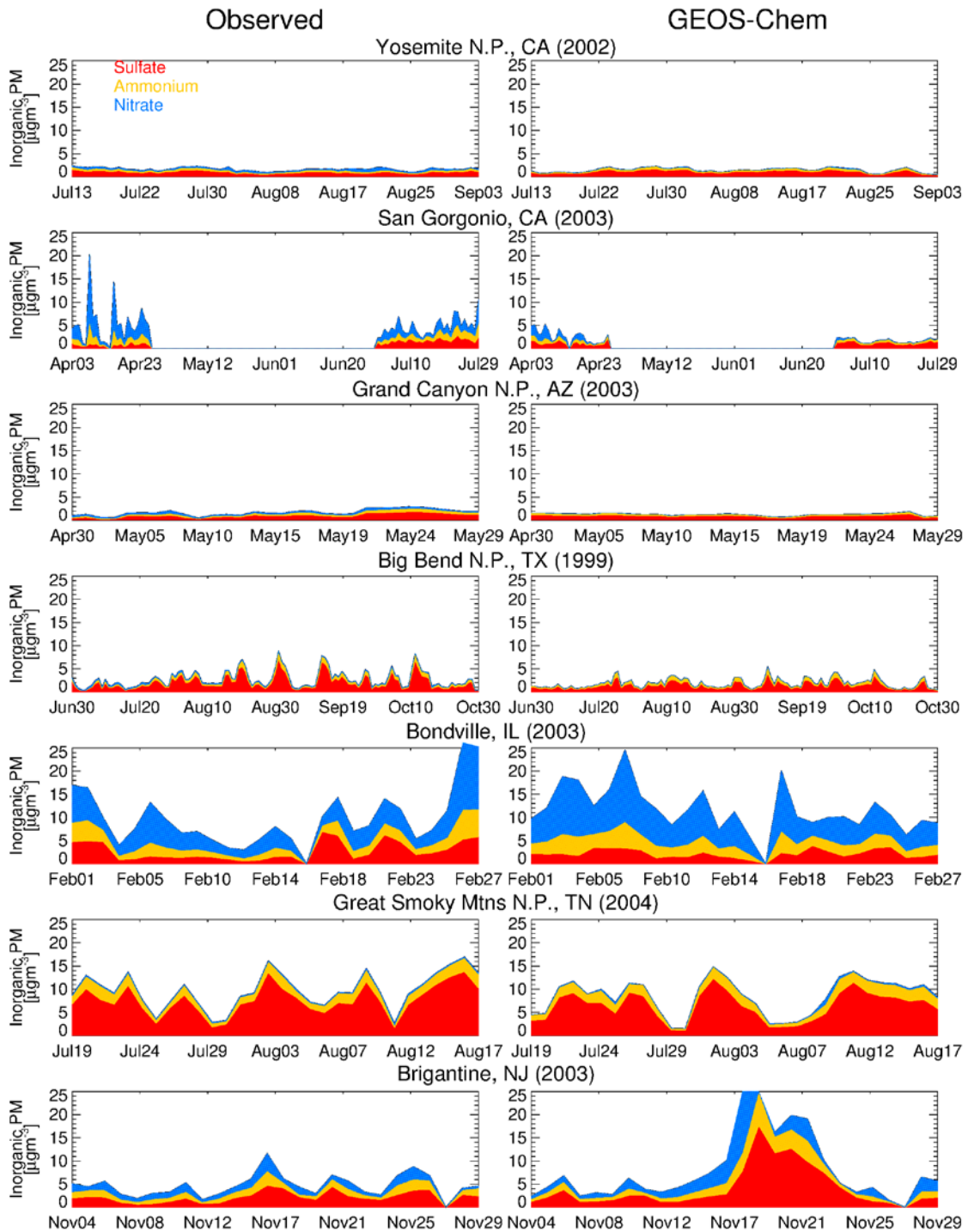
2 Figure 8: Annual mean concentrations of ammonia and speciated fine ammonium nitrate  
 3 during the Midwest Ammonia Monitoring Project in 2004. GEOS-Chem means (left=baseline  
 4 simulation, right=updated simulation) are shown with observed means overlaid.

5



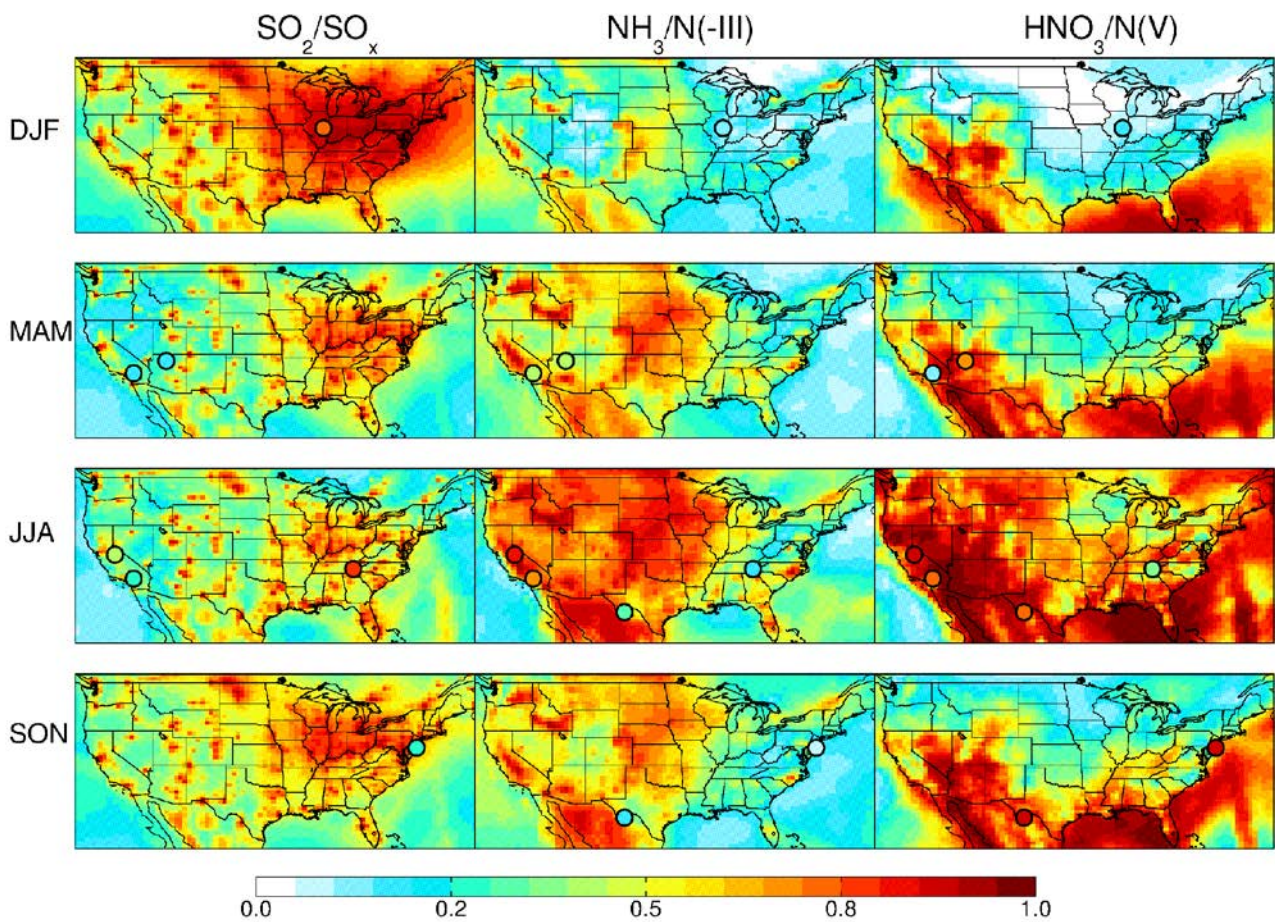
1

2 Figure 9: Timeseries of year-long monthly mean fine nitrate concentrations measured (black)  
 3 and simulated (red) in 2009 at 4 sites (from west to east): a) Boulder, WY, b) Rocky  
 4 Mountain National Park, CO, c) Loveland, CO and d) Brush, CO (solid). Standard deviation  
 5 of the individual observations averaged for each month shown as error bars.  
 6



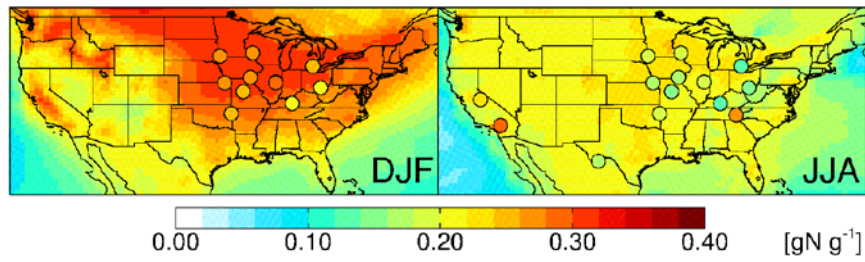
1  
2  
3  
4  
5

Figure 10: Timeseries of daily mean aerosol concentrations observed (left) and simulated (right) at the 7 focus sites. GEOS-Chem simulation is for 2004, years of measurements shown with site names.



1

2 Figure 11: Seasonal mean surface gas fractions simulated with GEOS-Chem for 2004. Mean  
 3 observations (from 1999, 2002, 2003 and 2004) overlaid on corresponding season. SO<sub>2</sub>  
 4 concentrations were not measured at the Big Bend National Park site (Section 2.2).  
 5



1

2 Figure 12: Fraction of nitrogen in winter (left) and summer (right) mean surface inorganic PM  
3 mass simulated with GEOS-Chem for 2004. Mean observations both from focus sites (from  
4 1999, 2002, 2003 and 2004) and 2004 MWNH3 campaign overlaid on corresponding season.